

ORIGINAL ARTICLE

# Neuregulin 1 signalling modulates mGluR1 function in mesencephalic dopaminergic neurons

A Ledonne<sup>1,2</sup>, A Nobili<sup>1</sup>, EC Latagliata<sup>1</sup>, V Cavallucci<sup>1</sup>, E Guatteo<sup>1</sup>, S Puglisi-Allegra<sup>1,3</sup>, M D'Amelio<sup>1,4</sup> and NB Mercuri<sup>1,2</sup>

Neuregulin 1 (NRG1) is a trophic factor that has an essential role in the nervous system by modulating neurodevelopment, neurotransmission and synaptic plasticity. Despite the evidence that NRG1 and its receptors, ErbB tyrosine kinases, are expressed in mesencephalic dopaminergic nuclei and their functional alterations are reported in schizophrenia and Parkinson's disease, the role of NRG1/ErbB signalling in dopaminergic neurons remains unclear. Here we found that NRG1 selectively increases the metabotropic glutamate receptor 1 (mGluR1)-activated currents by inducing synthesis and trafficking to membrane of functional receptors and stimulates phosphatidylinositol 3-kinase-Akt-mammalian target of rapamycin (PI3K-Akt-mTOR) pathway, which is required for mGluR1 function. Notably, an endogenous NRG1/ErbB tone is necessary to maintain mGluR1 function, by preserving its surface membrane expression in dopaminergic neurons. Consequently, it enables striatal mGluR1-induced dopamine outflow in *in vivo* conditions. Our results identify a novel role of NRG1 in the dopaminergic neurons, whose functional alteration might contribute to devastating diseases, such as schizophrenia and Parkinson's disease.

*Molecular Psychiatry* (2015) **20**, 959–973; doi:10.1038/mp.2014.109; published online 30 September 2014

## INTRODUCTION

Neuregulins (NRGs) are a family of trophic and differentiation factors that have an essential role in the development and function of the nervous system.<sup>1–4</sup> NRGs are encoded by four different genes (*NRG1–4*), of which *NRG1* is the best characterized. Different isoforms of NRG1s are produced by alternative splicing; they all share an epidermal growth factor (EGF)-like domain, which is essential for signalling transduction.<sup>1–4</sup> NRG1s are synthesized as membrane-anchored precursors, called pro-NRG1s, which undergo a proteolytic cleavage by different types of matrix metalloproteases, with the release of the diffusible active form in the extracellular compartment. NRG1s bind to receptor tyrosine kinases called ErbB, a family of proteins containing a single membrane-spanning segment. Four different subtypes of ErbB (ErbB1–4) have been characterized of which ErbB2, ErbB3 and ErbB4 mediate NRG1s signalling, whereas ErbB1 (also known as EGF receptor) is activated by EGF.

Binding of NRG1 induces the formation of homo and/or heterodimers of ErbB proteins, producing cross-phosphorylation of intracellular domains and activation of different signalling pathways, including phosphatidylinositol 3-kinase-Akt-mammalian target of rapamycin (PI3K-Akt-mTOR).<sup>4</sup>

Recent evidence suggests a role of NRG1/ErbB signalling in modulating the dopaminergic system.<sup>5</sup> It has been reported that NRG1 and different ErbB receptors subunits are strongly expressed in mesencephalic dopaminergic nuclei, both in the substantia nigra pars compacta (SNpc) and in the ventral tegmental area, from development to adulthood.<sup>6–9</sup> Moreover, a dysregulation of NRG1/ErbB signalling has been associated to brain disorders such as schizophrenia and Parkinson's disease (PD), in which an alteration of dopaminergic transmission has been clearly

demonstrated. In fact, *NRG1* is considered an important susceptibility gene for schizophrenia as several single-nucleotide polymorphisms have been reported in schizophrenic patients.<sup>4,10–13</sup> In line with this, alterations in the expression and signalling of NRG1/ErbB receptors have been reported in post-mortem studies of schizophrenic patients and in animal models of schizophrenia.<sup>14–19</sup> Of note, transgenic mice with altered NRG1/ErbB signalling show behavioural abnormalities related to the features of schizophrenia.<sup>9,20–25</sup> As NRG1s display a neuroprotective role in dopaminergic neurons in primary cultures<sup>26</sup> and PD animal model,<sup>27</sup> they have been proposed as crucial factors in the balance for life and death fate of these cells. This hypothesis has been corroborated by the evidence that ErbB4 receptors are overexpressed in residual dopaminergic neurons in PD patients,<sup>28</sup> suggesting that increased NRG1-mediated signalling could protect them from neuronal death.

Other experimental evidences also suggest a role of NRG1 in the modulation of dopaminergic system. For example, a transient exposure of mice to NRG1 in the neonatal period results in hyper-dopaminergic activity in the prefrontal cortex during adulthood.<sup>29</sup> Moreover, an alteration in the level of dopaminergic D2 receptors has been detected in transgenic mice hypomorphic for NRG1 in the striatum.<sup>30</sup> Furthermore, an intra-cerebral injection of NRG1 in rodents induces dopamine (DA) overflow both in the striatum<sup>31</sup> and in the hippocampus.<sup>32</sup>

At the cellular level, ErbB receptors appear preferentially localized in the postsynaptic densities (PSD), where they differently modulate the expression and/or the function of neurotransmitter receptors such as *N*-methyl-D-aspartate receptors (NMDARs),  $\alpha$ -amino-3-hydroxy-5-methylisoxazole-4-propionic acid receptors (AMPA), GABA<sub>A</sub>, nicotinic acetylcholine receptors and

<sup>1</sup>Department of Experimental Neurosciences, IRCCS Santa Lucia Foundation, Rome, Italy; <sup>2</sup>Department of Systems Medicine, University of Rome 'Tor Vergata', Rome, Italy; <sup>3</sup>Department of Psychology and 'Daniel Bovet' Center, University of Rome 'La Sapienza', Rome, Italy and <sup>4</sup>Laboratory of Molecular Neurosciences, Medical School University Campus-Biomedico, Rome, Italy. Correspondence: Dr A Ledonne or Professor NB Mercuri, Department of Experimental Neurosciences, IRCCS Santa Lucia Foundation, via del Fosso di Fiorano no. 64, Rome 00143, Italy or Professor M D'Amelio, Laboratory of Molecular Neurosciences, Medical School University Campus-Biomedico, via Alvaro del Portillo, 21, Rome 00128, Italy.

E-mail: adaledonne@virgilio.it or mercurin@med.uniroma2.it or m.damelio@unicampus.it

Received 13 May 2014; revised 1 July 2014; accepted 23 July 2014; published online 30 September 2014

metabotropic glutamate receptors (mGluRs),<sup>32–40</sup> thus regulating synaptic functions and plasticity.<sup>4</sup>

mGluR1 is highly expressed in mesencephalic dopaminergic neurons where it induces an increase in intracellular calcium,<sup>41</sup> an inward current mediated by canonical transient receptor potential (TRPC) channels,<sup>41,42</sup> an activation of burst firing discharge<sup>43</sup> and an increase in DA release in projection areas.<sup>44</sup> mGluR1 is also critically involved in neuronal development,<sup>45</sup> and in different forms of synaptic plasticity also associated with drugs of abuse,<sup>46–48</sup> and is implicated in several neuropsychiatric and neurodegenerative disorders.<sup>48,49</sup> These evidences prompted us to investigate whether NRG1/ErbB signalling affects mGluR1 activity in mesencephalic dopaminergic neurons.

Here we report a novel mechanism by which NRG1/ErbB tone regulates the strength of dopaminergic transmission by modulating mGluR1 expression and trafficking to membranes in the mesencephalic dopaminergic neurons thus affecting mGluR1-mediated functions both *in vitro* and *in vivo*.

## MATERIALS AND METHODS

### Slice preparation

All experiments were carried out in accordance with the international guidelines on the ethical use of animals from the European Communities Council Directive of 24 November 1986 (86/609/EEC) and the Comitato Etico of the Tor Vergata University, Rome, Italy. Acute midbrain slices were used to perform electrophysiology, immunofluorescence, biotinylation and biochemistry experiments.

To this end, Wistar rats (17–23-days old) were anesthetized with isoflurane and decapitated. The brain was rapidly removed from the skull, and a tissue block containing the midbrain was isolated and immersed in cold artificial cerebrospinal fluid (aCSF) at 8–10 °C. The aCSF contained (in mM): NaCl 126, KCl 2.5, MgCl<sub>2</sub> 1.2, CaCl<sub>2</sub> 2.4, NaH<sub>2</sub>PO<sub>4</sub> 1.2, NaHCO<sub>3</sub> 24, glucose 10, saturated with 95% O<sub>2</sub>–5% CO<sub>2</sub> (pH 7.4). Horizontal slices (200–250- $\mu$ m thick) of the ventral midbrain were cut using a vibratome (Leica VT1000S, Leica Microsystems, Wetzlar, Germany).<sup>50</sup> Slices were maintained in aCSF at 33.0  $\pm$  0.5 °C for 30 min before being differentially processed.

### Slice pharmacological treatments

After recovery from cutting procedure (30 min), midbrain slices were kept in a holding chamber containing standard aCSF, saturated with 95% O<sub>2</sub>–5% CO<sub>2</sub> at 33.5 °C and known concentration of drugs: NRG1 (5 nM; 5, 15 and 30 min), PD158780 (10  $\mu$ M, 15 min), PD158780+NRG1 (NRG1 5 nM, 30 min preceded by PD158780 10  $\mu$ M, 15 min), cycloheximide (CHX) (100  $\mu$ M, 1 h), CHX+NRG1 (CHX 100  $\mu$ M, 30 min followed by CHX 100  $\mu$ M plus NRG1 5 nM, 30 min), CPCCOEt (100  $\mu$ M, 30 min), CPCCOEt+NRG1 (CPCCOEt 100  $\mu$ M plus NRG1 5 nM, 30 min), MPEP (10  $\mu$ M, 30 min), MPEP+NRG1 (MPEP 10  $\mu$ M plus NRG1 5 nM, 30 min), anisomycin (ANISO) (40  $\mu$ M, 1 h) and ANISO+NRG1 (ANISO 40  $\mu$ M, 30 min followed by ANISO 40  $\mu$ M plus NRG1 5 nM, 30 min). Electrophysiological recordings on treated slices were performed within 30 min after the end of treatment. Immunofluorescence, biotinylation and biochemistry experiments were performed immediately at the end of slice pharmacological treatment.

### Electrophysiology

Whole-cell patch clamp recordings on dopaminergic neurons of SNpc were performed at 33.0  $\pm$  0.5 °C in a recording chamber placed on the stage of an upright microscope (Axioscope FS, Zeiss, Göttingen, Germany), equipped for infrared video microscopy (Hamamatsu, Tokyo, Japan). Slices were continuously perfused at 2.0–2.5 ml min<sup>-1</sup> with aCSF. SNpc neurons, visually selected by their localization and morphology, were identified as dopaminergic based on their electrophysiological properties (regular spontaneous firing at 0.5–4 Hz, presence of a large inward current ( $I_h$ ) in response to hyperpolarizing voltage steps) and response to application of DA (30  $\mu$ M) with membrane hyperpolarization/outward current.<sup>50</sup>

Whole-cell patch clamp recordings were performed with glass borosilicate pipettes (4–7 M $\Omega$ ) pulled with a PP 83 Narishige puller and filled with a solution containing (in mM): K<sub>2</sub>Gluconate 135, KCl 10, CaCl<sub>2</sub> 0.05, EGTA 0.1, Hepes 10, Na<sub>3</sub>-GTP 0.3, Mg-ATP 4 (pH 7.35 with KOH).

Cells were recorded in voltage-clamp mode ( $V_H = -60$  mV). Current signals were filtered at 3 kHz and digitized at 10 kHz using a Multiclamp 700A (Axon Instruments, Foster City, CA, USA) operated by the pClamp10 software (Molecular Devices, Sunnyvale, CA, USA). No series resistance compensation was implemented, in order to keep a low signal-to-noise ratio; however, recordings were discarded if series resistance changed by > 15% from control.

Amplitudes of membrane currents, induced by agonists, were calculated by measuring differences between baseline and peak and are expressed either as absolute values (pA) or percentage of controls.

Otherwise stated, drugs were bath applied at known concentrations via a three-way tap system. A complete exchange of the solution in the recording chamber occurred in about 1 min.

In the other set of experiments, (S)-3,5-dihydroxyphenylglycine ((S)-DHPG), AMPA and muscarine, dissolved in aCSF, were pressure applied (4–10 psi for 0.1–1.5 s), through a patch pipette connected to a Pneumatic Pico-pump PV 800 (WPI, Sarasota, FL, USA). The pipette was positioned above the slice in close proximity to the recorded neuron and agonists were applied every 3 min, to avoid receptor desensitization. Under these experimental conditions, stable and reproducible agonist-inward currents were recorded up to 2 h, before, during and after bath application of NRG1/ErbB signalling modulators.

### Immunofluorescence

Slices were fixed in 4% paraformaldehyde in 0.1 M phosphate buffer (PB) overnight at 4 °C and then immersed in 30% sucrose. Slices were cut into 30  $\mu$ m-thick sections by a freezing microtome and incubated overnight at 4 °C with primary antibodies diluted in PB containing 0.3% Triton X-100. After three washes in PB, sections were incubated for 2 h with secondary antibodies. After three washes in PB, sections were mounted on slides, air-dried and coverslipped with Fluoromount (Sigma Aldrich, Milan, Italy). Double fluorescence was examined under a confocal scanning laser microscope (ZEISS, LSM700, Oberkochen, Germany).

Primary antibodies were: mGluR1 (1:200, Santa Cruz, Dallas, TX, USA; sc-99040), and TH (1:400, Santa Cruz sc-7847). Secondary antibodies were: Alexa Fluor 488 donkey anti-goat immunoglobulin G (1:200, Life Technologies, Carlsbad, CA, USA; A-11055), and Alexa Fluor 555 donkey anti-rabbit immunoglobulin G (1:200, Life Technologies A-21428).

### Densitometric analyses of fluorescence images

Quantification of the changes in the IR mGluR1 signal due to different treatment is performed on TH/mGluR1-positive cells by densitometric analyses. After background subtraction, mGluR1 cell-associated signals were quantified by manually outlining individual cells and measuring cell-associated fluorescence intensity with the ImageJ software (<http://rsb.info.nih.gov/ij/>). The ratio defines mean fluorescence of individual cells normalized to total cellular surface. Quantification was done in blind on 200 cells per group ( $n = 3$  rats per group).

All data were expressed as means  $\pm$  s.d. and represented as a percentage of control.

### Slice biotinylation

Surface biotinylation was performed as previously described,<sup>51</sup> with little modifications. For each experiment (three independent experiments), four rats were used and slices equally distributed per each experimental condition. Midbrain slices (200  $\mu$ m) were incubated in standard aCSF saturated with 95% O<sub>2</sub> and 5% CO<sub>2</sub>, containing 0.5 mg ml<sup>-1</sup> sulpho-NHS-LC-Biotin (Pierce, Rockford, IL, USA) for 1 h on ice. After the biotinylation, the SNpc was quickly isolated from the slices by manual dissection by using a hypodermic needle under a microscope (Axioscope FS, Zeiss, Göttingen, Germany) and then washed once with ice-cold aCSF, followed by two washes in ice-cold TBS (50 mM Tris, pH 7.5, 150 mM NaCl). Slices were homogenized in Homogenization Buffer (1% Triton X-100, 0.1% sodium dodecyl sulphate, 50 mM Tris-HCl (pH 7.5), 0.3 M Sucrose, 5 mM EDTA, 0.5 mM sodium orthovanadate, 5 mM  $\beta$ -glycerophosphate, protease inhibitor cocktail—Sigma P8340) and then briefly sonicated. Homogenized samples were centrifuged at 13 000 g for 10 min at 4 °C, and the total protein content of resulting supernatant was measured by Bradford method. For each sample, we obtained about 350  $\mu$ g protein: 25  $\mu$ g protein was probed for TH content as a marker of the DAergic neurons population, and equal aliquots of biotinylated lysates (300  $\mu$ g protein) were incubated with NeutrAvidinagarose (Pierce) in a 1:1 ratio for 16 h at 4 °C. Biotinylated proteins attached to NeutrAvidin-coated beads were separated by

centrifugation (1000 *g* for 1 min at 4 °C). The beads were washed two times with Wash Buffer (Pierce), and the bound proteins were eluted with sodium dodecyl sulphate sample buffer by boiling it for 10 min.

#### Protein extraction from SNpc

For each experiment (three independent experiments), two rats were used, and slices were equally distributed per experimental condition. After the treatment, SNpc was quickly isolated from slices, and three samples per group were pooled for protein extraction. Samples were homogenized in lysis buffer (320 mM sucrose, 50 mM NaCl, 50 mM Tris-HCl (pH 7.5), 1% Triton X-100, 1 mM sodium orthovanadate, 5 mM  $\beta$ -glycerophosphate, 5 mM NaF, protease inhibitor cocktail), incubated on ice for 30 min and centrifuged at 13 000 *g* for 10 min. The total protein content of the resulting supernatant was determined by Bradford method.

#### Immunoblotting analysis and antibodies

Proteins were applied to sodium dodecyl sulphate-polyacrylamide gel electrophoresis and electroblotted on a polyvinylidene difluoride membrane. Immunoblotting analysis was performed using a chemiluminescence detection kit. The relative levels of immunoreactivity were determined by densitometry using the ImageJ software. Significance was tested using one-way analysis of variance (ANOVA) with a Bonferroni's *post-hoc* test. All statistical analyses were performed using the Prism-4 software (GraphPad Software, San Diego, CA, USA), with the significance level set at  $P < 0.05$ .

Primary antibodies were: ErbB4 (1:200, Santa Cruz sc-283), phospho-ErbB4 (1:300, Cell Signaling, Danvers, MA, USA; no.4754), Akt1 (1:1000, Cell Signaling no.2938), phospho-Akt (1:1000, Cell Signaling no.9271), mTOR (1:2000, Cell Signaling no.2972), phospho-mTOR (1:2000, Cell Signaling no.2971), eukaryotic elongation factor 2 (eEF2) (1:1000, Sigma Aldrich SAB4500695), mGluR1 (1:300, Santa Cruz sc-99040), mGluR5 (1:1000, Abcam, Cambridge, UK; ab76316), GluR1 (1:1000, Millipore, Darmstadt, Germany; 04-855), NR2B (1:1000, Millipore no.06-600), TH (1:1000, Santa Cruz sc-14007), actin (1:25 000, Sigma Aldrich A5060). Secondary antibody was: goat anti-rabbit immunoglobulin G (1:3000, Bio-Rad, Hercules, CA, USA; 170-6515).

#### Microdialysis

Male Wistar rats (300–400 g) were housed in groups of three per cage with food and water *ad libitum* in animal facility where temperature was kept between 22 and 23 °C and lights were on from 0700 to 1700 hours. All surgery and experiments were carried out between 1100 and 1800 hours. Surgeries were performed 52–48 h before experiments. Rats, anesthetized with Zoletil 100 (Tiletamine HCl 50 mg ml<sup>-1</sup>+Zolazepam HCl 50 mg ml<sup>-1</sup>) and Rompun (Xylazine 20 mg ml<sup>-1</sup>), were mounted on a stereotaxic frame (David Kopf Instruments, Tujunga, CA, USA) and implanted unilaterally, following the coordinates of Paxinos and Watson,<sup>52</sup> with concentric microdialysis probes at the level of striatum and with 22-gauge, 7mm-long stainless steel guide cannula at the level of ipsilateral SNpc (coordinates: striatum = A: +0.6, L: 2.8 from bregma, V: -6.5; SNpc = A: -5, L: 1.2 from bregma, V: -0.3). Vertical concentric dialysis probes, with a length of dialysing portion of 2 mm, were prepared with AN69 fibres (Hospal Dasco, Bologna, Italy). Each probe and cannula were fixed with epoxy glue and dental cement, and the skin was sutured. At the end of surgery, animals were housed individually into a new home cage to avoid the breaking of the implantation. On the day of experiment, rats were introduced to individual testing cages, similar in shape and measures to standard housing cages. The microdialysis probe was connected to a CMA/100 pump (Carnegie Medicine, Stockholm, Sweden) through PE-20 tubing and an ultralow torque multi-channel power assisted swivel (Model MCS5, Instech Laboratories, Inc., Plymouth Meeting, PA, USA) to allow free movement. aCSF (in mM: NaCl 140.0; KCl 4.0; CaCl<sub>2</sub> 1.2; MgCl<sub>2</sub> 1.0) was pumped through the dialysis probe at a constant flow rate of 2.1  $\mu$ l min<sup>-1</sup>. Following the start of the dialysis perfusion, rats were left undisturbed for approximately 1 h before the collection of baseline samples. The mean concentration of the three samples collected immediately before treatment (< 10% variation) was taken as the basal concentration.

After collection of basal samples, 1  $\mu$ l per 2 min of vehicle (aCSF plus dimethyl sulphoxide), CPCCOEt (10 mM) or PD158780 (10  $\mu$ M) was injected into SNpc through a stainless-steel cannula (0.15 mm OD; 16 mm length; UNIMED, Switzerland) connected to a 10- $\mu$ l syringe by a polyethylene tube and driven by a CMA/100 pump.

Thirty minutes after the first injection, all rats received another injection of 1  $\mu$ l per 2 min of DHPG (5 mM), DHPG (5 mM) plus CPCCOEt (10 mM), DHPG (5 mM) plus PD158780 (10  $\mu$ M), vehicle, CPCCOEt (10 mM) or PD158780 (10  $\mu$ M) by the same system. The dialysate samples were collected every 10 min for 90 min and brought to a volume of 42  $\mu$ l by adding 21  $\mu$ l of aCSF. Placements in striatum and SNpc were judged by methylene blue staining. Only data from rats with correctly placed probe and cannula have been reported. Concentrations (pg per 10  $\mu$ l) were not corrected for probe recovery. The UPLC system consisted of an Acquity UPLC (Waters Corporation, Milford, MA, USA) apparatus coupled to an amperometric detector (model Decade II, Antec Leyden, The Netherlands), as previously described.<sup>53</sup> The detection limit of assay was 0.1 pg.

#### Drugs

NRG1 $\beta$ 1 (EGF-like domain), rapamycin, (+)-muscarine chloride, cycloheximide, anisomycin (ANISO) and isoflurane were purchased from Sigma-Aldrich. (S)-DHPG, AMPA, NMDA, CPCCOEt and MPEP were obtained from Ascent Scientific (Bristol, UK).

PD158780, AG879, AG1478 hydrochloride, LY294002, Wortmannin and Dynasore were purchased from Tocris Cookson Inc. (Bristol, UK). GM6001 was obtained from Santa Cruz Biotechnology.

Zoletil 100 (Tiletamine HCl 50 mg ml<sup>-1</sup>+ Zolazepam HCl 50 mg ml<sup>-1</sup>) was purchased from Virbac, (Milano, Italy) and Rompun 20 (Xylazine 20 mg ml<sup>-1</sup>) was obtained from Bayer S.p.A (Milano, Italy).

#### Statistical analysis

Numerical data were expressed as mean  $\pm$  s.e.m. or s.d. Statistical comparisons of data obtained from electrophysiological experiments were performed using the Student's *t*-test (paired or unpaired data) or with one-way ANOVA followed by *post-hoc* Holm-Sidak test. In immunofluorescence experiments and immunoblotting analysis, significance was tested using one-way ANOVA with a Bonferroni's *post-hoc* test.

In microdialysis experiments, statistical analyses were carried out on raw data, and analysed by repeated-measures ANOVA with one between factor (treatment, 3 levels: Veh+DHPG, CPCCOEt+DHPG; PD158780+DHPG) and one within factor (time, 10 levels: 0, 10, 20, 30, 40, 50, 60, 70, 80, 90 min). Simple effect of treatment was assessed by one-way ANOVA on data from samples collected at each time point. The minimal level of statistical significance was set at  $P < 0.05$ .

## RESULTS

### NRG1 potentiates mGluR1-activated currents

We have previously reported that the group I mGluR agonist (S)-DHPG evokes an inward current in SNpc dopaminergic neurons, which is mainly mediated by mGluR1 subtype inducing the activation of TRPC channels.<sup>40,41</sup> In order to investigate the effect of ErbB activation on mGluR1 function, we compared the amplitudes of (S)-DHPG-activated currents (10  $\mu$ M; 3 min, bath applied) in DAergic cells from midbrain slices treated with NRG1 (5 nM, 30 min) with those recorded in untreated slices (controls). We found that NRG1 treatment determined a significant enhancement of the (S)-DHPG-activated currents (Figure 1a), from  $-104.08 \pm 15.88$  pA (control) to  $-173.75 \pm 18.45$  pA in NRG1-treated slices ( $P < 0.05$ , CTR ( $n = 17$ ) vs NRG1 ( $n = 13$ ), one-way ANOVA followed by Holm-Sidak test) (Figure 1b).

To confirm the involvement of mGluR1 receptors in the (S)-DHPG-induced responses potentiated by NRG1, we compared the amplitude of (S)-DHPG-activated currents in midbrain slices treated with the selective mGluR1 antagonist, CPCCOEt (100  $\mu$ M, 30 min) alone and in the presence of NRG1 (5 nM, 30 min). We found that CPCCOEt treatment *per se* strongly reduced (S)-DHPG-activated currents ( $n = 9$ ;  $P < 0.001$  CPCCOEt vs CTR) and completely counteracted the NRG1 enhancing effect ( $P < 0.001$ , CPCCOEt+NRG1 ( $n = 9$ ) vs NRG1 ( $n = 13$ ), one-way ANOVA followed by Holm-Sidak test; Figures 1a and b).

As (S)-DHPG is an agonist for group I mGluR also activating mGluR5 besides mGluR1,<sup>54</sup> the NRG1-induced increase in (S)-DHPG-activated currents might be partially dependent on a mGluR5-mediated mechanism. Notably, in midbrain slices treated with the

selective mGluR5 antagonist, MPEP (10  $\mu\text{M}$ , 30 min), the (S)-DHPG-activated currents were slightly reduced ( $n=14$ ,  $P < 0.05$ , MPEP vs CTR) but a treatment with NRG1 (5 nM, 30 min) in the presence of MPEP still induced a significant enhancement of the (S)-DHPG-induced responses ( $n=12$ ,  $P < 0.05$ , MPEP+NRG1 vs MPEP, one-way ANOVA followed by Holm–Sidak test; Figures 1a and b).

To explore the time course of NRG1 effect on (S)-DHPG-activated currents, we performed long lasting recordings in which (S)-DHPG (100–300  $\mu\text{M}$ ) was locally applied by pressure ejection every 3 min onto the recorded neuron (see Materials and methods) and NRG1 was bath applied (5 nM, 12 min). Also, under these conditions, NRG1 produced a significant increase of

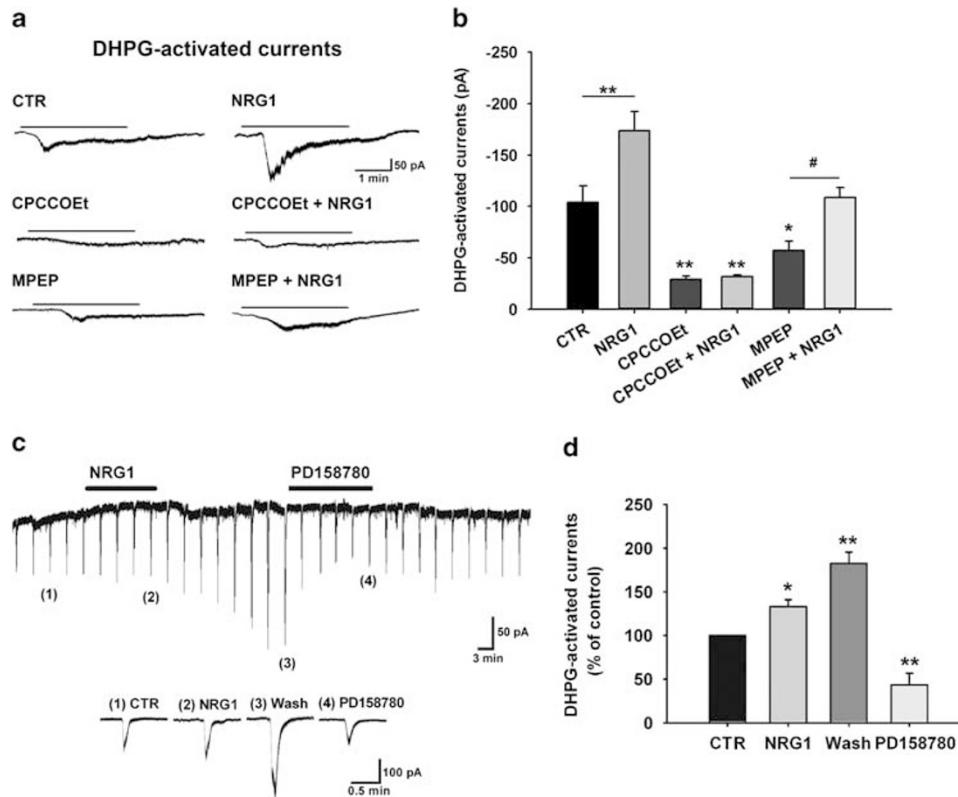
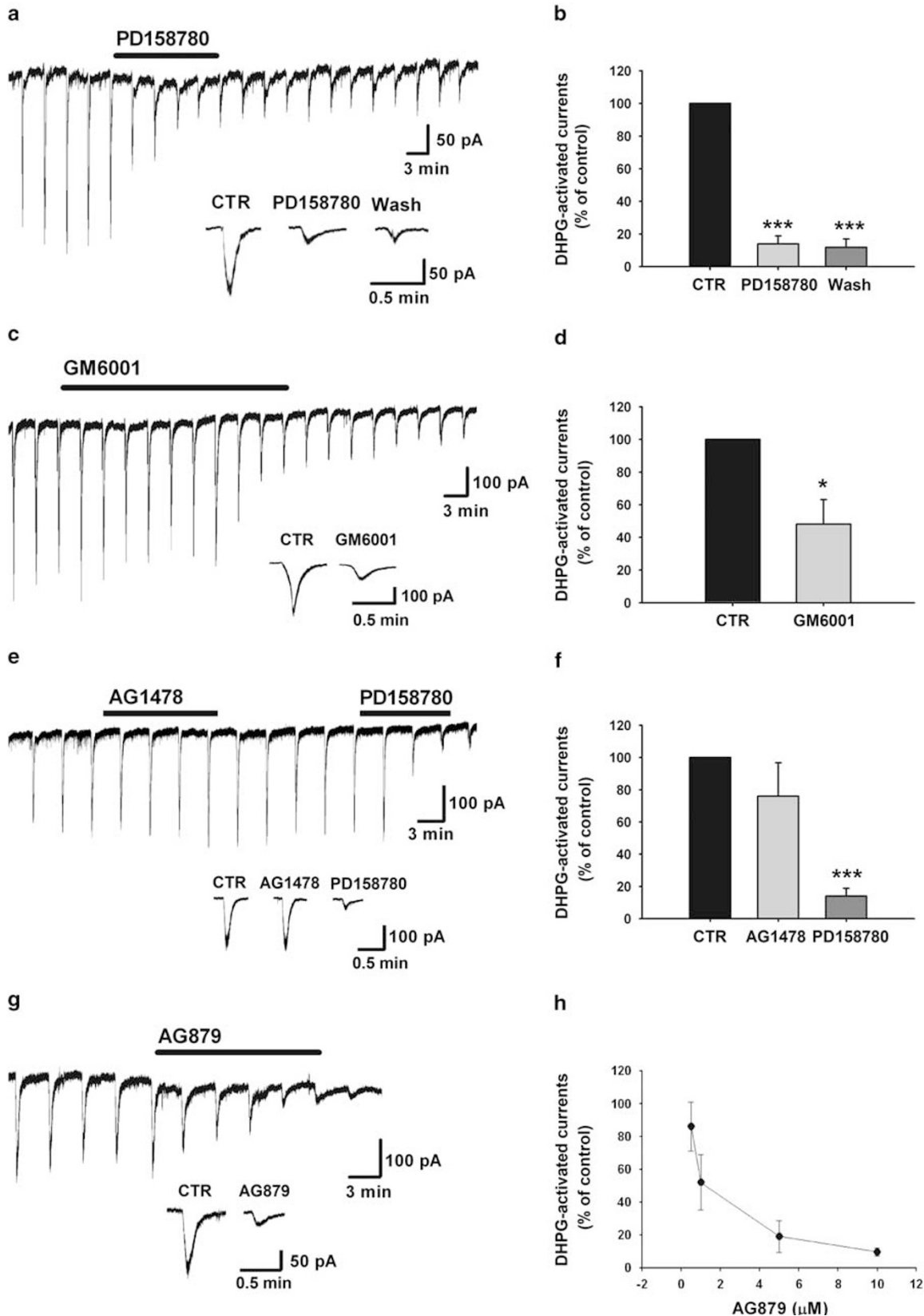


**Figure 1.** Neuregulin 1 (NRG1)-induced upregulation of metabotropic glutamate receptor 1 (mGluR1)-activated currents. **(a)** Representative electrophysiological traces showing inward currents induced by bath application of (S)-3,5-dihydroxyphenylglycine ((S)-DHPG) (10  $\mu\text{M}$ , 3 min) in substantia nigra pars compacta dopaminergic neurons of midbrain slices in control conditions and following different pharmacological treatments: NRG1 (5 nM, 30 min), CPCCOEt (100  $\mu\text{M}$ , 30 min), CPCCOEt+NRG1 (CPCCOEt 100  $\mu\text{M}$  plus NRG1 5 nM, 30 min), MPEP (10  $\mu\text{M}$ , 30 min), and MPEP+NRG1 (MPEP 10  $\mu\text{M}$  plus NRG1 5 nM, 30 min). **(b)** Histogram showing mean amplitudes of (S)-DHPG-activated currents (pA) in the various pharmacological conditions: CTR ( $n=17$ ), NRG1 ( $n=13$ ), CPCCOEt ( $n=10$ ), CPCCOEt+NRG1 ( $n=10$ ), MPEP ( $n=14$ ), and MPEP+NRG1 ( $n=12$ );  $*P < 0.05$ ,  $**P < 0.01$ ,  $***P < 0.001$  vs CTR;  $\#P < 0.05$  MPEP vs MPEP+NRG1, one-way analysis of variance followed by Holm–Sidak test). **(c)** Representative electrophysiological recording showing the acute effect of NRG1 (5 nM) on mGluR1-activated currents induced by repetitive pressure application of (S)-DHPG (100  $\mu\text{M}$ , 1 s) every 3 min near to the recorded neuron. Below: Enlargements of (S)-DHPG-activated currents at the indicated numbers: (1) CTR, (2) NRG1 (5 nM, 12 min); (3) Wash (24–30 min after NRG1 has been stopped), and (4) PD158780 (10  $\mu\text{M}$ , 15 min). **(d)** Histogram showing normalized (S)-DHPG-activated currents (expressed as percentage of control) in the different conditions reported in panel (c) ( $*P < 0.05$ ,  $**P < 0.01$ , paired  $t$ -test).

**Figure 2.** Endogenous Neuregulin 1/ErbB signalling is necessary for metabotropic glutamate receptor 1 (mGluR1) function. **(a)** Representative electrophysiological trace showing the effect of PD158780 (10  $\mu\text{M}$ ) on mGluR1-activated currents induced by repetitive pressure application of (S)-DHPG (100  $\mu\text{M}$ , 1.5 s). Below: Enlargements of (S)-3,5-dihydroxyphenylglycine ((S)-DHPG)-activated currents before (CTR), during PD158780 (10  $\mu\text{M}$ ; 15 min) and 30 min after PD158780 has been stopped (wash). **(b)** Histogram showing mean amplitudes of (S)-DHPG-activated currents (percentage of control) in the different pharmacological conditions reported in panel (a). Notably, PD158780 effect did not wash out ( $n=7$ ,  $***P < 0.001$ , paired  $t$ -test). **(c and d)** Effect of GM6001, a broad-spectrum matrix metalloprotease inhibitor, on mGluR1-activated currents. As reported in the representative trace shown in panel (c) and in the histogram showing mean amplitudes of (S)-DHPG-activated currents (percentage of control) in panel (d), bath application of GM6001 (25  $\mu\text{M}$ , 30 min) gradually reduces mGluR1-induced currents ( $n=5$ ,  $*P < 0.05$ , paired  $t$ -test). **(e and f)** Effect of the ErbB1 inhibitor AG1478 on mGluR1-activated currents. Representative trace **(e)** and mean values **(f)** of (S)-DHPG-activated currents amplitudes (percentage of control) showing the effect of the ErbB1 inhibitor AG1478 (10  $\mu\text{M}$ ,  $n=5$ ,  $P > 0.05$ , paired  $t$ -test) and PD158780 (10  $\mu\text{M}$ ,  $n=5$ ,  $***P < 0.001$ , paired  $t$ -test) on inward currents induced by pressure application of (S)-DHPG (100  $\mu\text{M}$ , 1 s). **(g)** Representative trace showing the effect of the selective ErbB2 inhibitor AG879 (10  $\mu\text{M}$ ) on mGluR1-activated currents, induced by pressure application of (S)-DHPG (100  $\mu\text{M}$ , 1.5 s). **(h)** Concentration–response curve of the effect of AG879 on (S)-DHPG-activated currents (expressed as percentage of control) ( $n=6$  for each concentration).

(S)-DHPG-activated currents (Figure 1c) up to  $132.94 \pm 8.09\%$  of control ( $n=6$ ,  $P < 0.05$ , paired *t*-test). This effect had a late onset, as it started at the end of NRG1 application and continued during NRG1 washout reaching a maximal increase to  $182.58 \pm 12.81\%$  of control ( $n=6$ ,  $P < 0.01$ , paired *t*-test) after 24–30 min (Figure 1d).

Interestingly, the NRG1-induced increase of the (S)-DHPG-activated currents was strongly reduced by the application of the broad-spectrum inhibitor of ErbB receptors, PD158780 ( $10 \mu\text{M}$ , 15 min), supporting the involvement of ErbB activation in the NRG1-mediated effects (Figure 1d).



### Endogenous NRG1/ErbB signalling is necessary to mGluR1 function

To further unravel the role of the NRG1/ErbB signalling in the modulation of mGluR1 function, we investigated whether an endogenous NRG1 tone is required for the proper mGluR1 functioning.

To this end, we prevented endogenous ErbB activation by using PD158780 (10  $\mu\text{M}$ , 15 min) and tested its effect on (S)-DHPG-activated currents, in the absence of exogenous NRG1.

Interestingly, when applied alone PD158780 produced a dramatic reduction of the (S)-DHPG-activated currents (Figure 2a), supporting a role of endogenous NRG1 in the maintenance of mGluR1 activity. In particular, the (S)-DHPG-activated currents were decreased to  $13.95 \pm 4.93\%$  of control ( $n=7$ ;  $P < 0.001$ ; paired  $t$ -test), with no recovery up to 30 min of washout of the ErbB inhibitor. Indeed, the (S)-DHPG-induced currents were still reduced to  $11.77 \pm 5.23\%$  of control after 30 min of PD158780 washout ( $n=7$ ;  $P < 0.001$ ; paired  $t$ -test; Figure 2b).

To further investigate the role of endogenous NRG1 in the modulation of mGluR1 function, we interfered with NRG1 synthesis. To this purpose, we used a broad-spectrum matrix metalloprotease inhibitor, GM6001, and evaluated its effect on mGluR1-activated currents. Bath superfusion of GM6001 (25  $\mu\text{M}$ , 30 min) gradually reduced (S)-DHPG-activated currents to  $48.16 \pm 14.93\%$  of control ( $n=5$ ,  $P < 0.05$ , paired  $t$ -test; Figures 2c and d). These results confirm that endogenous NRG1/ErbB signalling is indispensable to mGluR1 functioning.

### Subunit composition of ErbB receptors is involved in the modulation of mGluR1-activated currents

NRG1 could activate different types of ErbB receptors made up of specific combinations of ErbB proteins (ErbB2, ErbB3, ErbB4) to elicit an effect on mGluR1-activated currents. In order to assess the subunit composition of ErbB dimers activated by endogenous NRG1, we recorded (S)-DHPG-activated currents in the presence of different subunit-specific ErbB inhibitors.

The involvement of ErbB1 receptor has been excluded by using the selective ErbB1 inhibitor, AG1478. In fact, in the presence of AG1478 (10  $\mu\text{M}$ , 15 min) (S)-DHPG-activated currents were not significantly modified, being  $75.93 \pm 20.67\%$  of control ( $n=5$ ;  $P > 0.05$ , paired  $t$ -test). Notably, the AG1478-insensitive currents were still inhibited by the pan-ErbB inhibitor PD158780 (Figures 2e and f). By contrast, in the presence of AG879, a selective ErbB2 receptors inhibitor, the mGluR1-activated responses were strongly inhibited. In particular, in the presence of AG879 (10  $\mu\text{M}$ , 9 min) (S)-DHPG-activated currents were reduced to  $9.19 \pm 2.73\%$  of control ( $n=11$ ,  $P < 0.001$ , paired  $t$ -test) (Figures 2g and h). The depressant effect induced by AG879 on (S)-DHPG-activated currents was concentration dependent (Figure 2h).

### NRG1/ErbB signalling selectively modulates mGluR1-activated currents

Recent evidence has demonstrated that NRG1 modulates the glutamatergic ionotropic responses mediated by AMPA and NMDA receptors in different brain areas.<sup>32,37,38</sup> To this regard, we tested whether the NRG1/ErbB signalling, beside affecting mGluR1-activated currents, modulates ionotropic glutamate receptor-induced responses in SNpc dopaminergic neurons.

We found that NRG1 did not modify the NMDA-activated currents (Figure 3a). Indeed, in slices treated with NRG1 (5 nM, 30 min), the amplitude of inward currents induced by NMDA (50  $\mu\text{M}$ , 45 s) was  $-195.77 \pm 21.16$  pA ( $n=11$ ), whereas in untreated slices (control) it was  $-222.22 \pm 12.44$  pA ( $n=11$ ,  $P > 0.05$ , unpaired  $t$ -test; Figure 3a). In addition, an endogenous NRG1 tone did not affect NMDA receptor function as NMDA-activated currents were unchanged by PD158780 (10  $\mu\text{M}$ , 15 min) ( $95.92 \pm 6.59\%$  of control;  $n=5$ ,  $P > 0.05$ , paired  $t$ -test; Figure 3b).

Similarly, NRG1/ErbB signalling did not modulate AMPAR-mediated currents in SNpc dopaminergic neurons. In fact, in slices treated with NRG1 (5 nM, 30 min) the mean amplitude of inward currents induced by AMPA (10  $\mu\text{M}$ , 10 s) was  $-307.99 \pm 38.71$  pA ( $n=10$ ) while in untreated slices (control) it was  $-356.72 \pm 43.14$  pA ( $n=10$ ,  $P > 0.05$ , unpaired  $t$ -test) (Figure 3c). Furthermore, ErbB inhibition with PD158780 (10  $\mu\text{M}$ , 15 min) did not modify AMPA-activated currents ( $95.92 \pm 6.59\%$  of control,  $n=5$ ;  $P > 0.05$ ; paired  $t$ -test) produced by pressure applications of AMPA (100  $\mu\text{M}$ , 2–10 psi, 0.1 s; Figure 3d).

It is known that the inward currents induced by mGluR1 stimulation in SNpc dopaminergic neurons are mediated by TRPC channels,<sup>42</sup> which can be also gated by other G-protein coupled receptors (GPCRs), linked to Gq proteins, such as M1–M3 muscarinic receptors.<sup>55</sup> To test whether the modulatory effect of NRG1/ErbB signalling on mGluR1-activated responses might be due to an action on GPCRs/TRPC channels, we analysed the muscarine-activated currents. We found that slice treatment with NRG1 (5 nM, 30 min) did not significantly modify the muscarine-induced responses (Figure 3e). The mean amplitudes of inward currents activated by muscarine (30  $\mu\text{M}$ , 2 min) were  $-46.78 \pm 5.43$  pA in NRG1-treated slices ( $n=10$ ) and  $-46.92 \pm 6.04$  pA in untreated slices (control) ( $n=9$ ,  $P > 0.05$ , unpaired  $t$ -test). Moreover, an endogenous tone of NRG1 was not essential for the muscarinic activity, as in the presence of PD158780 (10  $\mu\text{M}$ ; 15 min) the inward current produced by locally applied muscarine (300  $\mu\text{M}$ , 2–10 psi, 0.5–1 s) was  $94.65 \pm 6.94\%$  of control ( $n=5$ ,  $P > 0.05$ ; paired  $t$ -test) (Figure 3f).

Collectively, these experiments demonstrate that NRG1/ErbB signalling selectively modulates mGluR1-mediated responses in the dopaminergic neurons of SNpc, whereas both the ionotropic glutamatergic and the cholinergic muscarinic transmissions were largely unaffected.

### NRG1/ErbB signalling regulates mGluR1 expression

Next, we aimed at understanding the molecular mechanism by which NRG1 determines the increase of mGluR1-activated responses. One possibility was that the NRG1-induced upregulation of mGluR1-activated currents was dependent on *de novo* protein synthesis. Therefore we analysed the effect of NRG1 on (S)-DHPG-activated currents in the presence of two different inhibitors of protein synthesis, CHX and ANISO.

Interestingly, CHX prevented NRG1-induced increase of mGluR1-activated currents (Figures 4a and b). In fact, in CHX-treated slices (100  $\mu\text{M}$ ) treatment with NRG1 (5 nM; 30 min) was not able to modify (S)-DHPG-activated currents, whose amplitude was  $-108.07 \pm 18.95$  pA ( $n=11$ ,  $P > 0.05$ , CHX+NRG1 vs CTR, one-way ANOVA followed by Holm–Sidak test). Similarly ANISO completely counteracted NRG1-induced increase of (S)-DHPG-activated currents, whose amplitude was  $-58.48 \pm 7.28$  pA ( $n=10$ ,  $P > 0.05$ , ANISO+NRG1 vs CTR, one-way ANOVA followed by Holm–Sidak test).

Treatments with either CHX and ANISO *per se* did not affect the amplitudes of mGluR1-activated currents, which were  $-79.50 \pm 12.90$  pA in CHX-treated slices ( $n=11$ ,  $P > 0.05$ , CHX vs CTR; one-way ANOVA followed by Holm–Sidak test) and  $-63.28 \pm 8.80$  pA in ANISO-treated slices ( $n=10$ ,  $P > 0.05$  ANISO vs CTR; one-way ANOVA followed by Holm–Sidak test) (Figure 4b).

To verify whether the upregulation of mGluR1-activated currents by NRG1 was due to an increase of mGluR1 expression, we performed a confocal microscope analysis of SNpc DAergic neurons in midbrain slices double-labelled for TH (green) and mGluR1 (red) (Figure 4c). NRG1 application (5 nM, 30 min) induced a strong increase of mGluR1 staining compared with controls ( $173.9 \pm 27.65\%$  of control). This effect was completely abolished by either PD158780 or CHX or ANISO (Figures 4c and d), demonstrating that the NRG1-induced increase of mGluR1

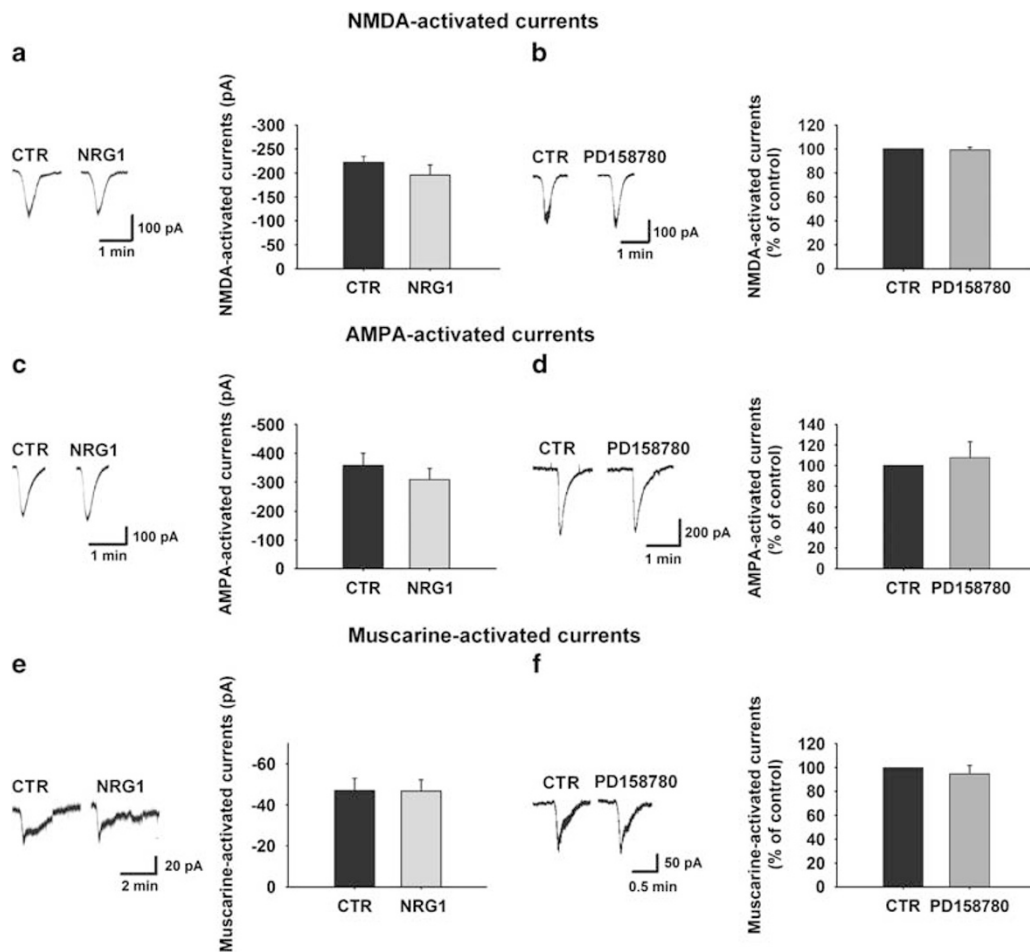


**Figure 3.** Neuregulin 1 (NRG1)/ErbB signalling selectively modulates metabotropic glutamate receptor 1-activated responses. **(a and b)** Effect of NRG1/ErbB signalling on *N*-methyl-D-aspartate (NMDA)-activated currents. **(a)** Example traces (left) and mean current amplitudes (pA) (right) induced by NMDA ( $50 \mu\text{M}$ , 45 s, every 4 min) in control and in NRG1-treated slices ( $5 \text{ nM}$ , 30 min) ( $n = 11$  each condition,  $P > 0.05$ , unpaired *t*-test). **(b)** Example traces (left) and mean current amplitudes (percentage of control) (right) of the inward currents elicited by NMDA ( $50 \mu\text{M}$ , 45 s, every 4 min) before and during bath application of PD158780 ( $10 \mu\text{M}$ , 15 min) ( $n = 5$ ,  $P > 0.05$ , paired *t*-test). **(c and d)** Effect of NRG1/ErbB signalling on  $\alpha$ -amino-3-hydroxy-5-methylisoxazole-4-propionic acid (AMPA)-activated currents. **(c)** Example traces (left) and mean current amplitudes (pA) (right) of the inward currents induced by AMPA ( $10 \mu\text{M}$ , 10 s) in control and NRG1-treated slices ( $5 \text{ nM}$ , 30 min) ( $n = 10$  each condition,  $P > 0.05$ , unpaired *t*-test). **(d)** Example traces (left) and mean current amplitudes (percentage of control) (right) of the inward currents produced by pressure-applied AMPA ( $100 \mu\text{M}$ , 0.1 s, every 3 min) before and during bath application of PD158780 ( $10 \mu\text{M}$ , 15 min) ( $n = 5$ ,  $P > 0.05$ , paired *t*-test). **(e and f)** Effect of NRG1/ErbB signalling on muscarine-activated currents. **(e)** Example traces (left) and mean current amplitudes (pA) (right) of inward currents elicited by muscarine ( $30 \mu\text{M}$ , 2 min) in control and NRG1-treated slices ( $5 \text{ nM}$ , 30 min) ( $n = 10$  each condition,  $P > 0.05$ , unpaired *t*-test). **(f)** Example traces (left) and mean current amplitudes (percentage of control) (right) of the inward currents induced by pressure-applied muscarine ( $300 \mu\text{M}$ , 1 s, every 3 min) before and during bath application of PD158780 ( $10 \mu\text{M}$ , 15 min) ( $n = 5$ ,  $P > 0.05$ , paired *t*-test).

staining was dependent on activation of ErbB receptors and required new protein synthesis. Exposure to PD158780, CHX or ANISO, in the absence of NRG1, did not alter the mGluR1 staining intensity, suggesting that their inhibitory effect was restricted to protein synthesis induced by NRG1 application.

NRG1 activates PI3K-Akt-mTOR pathway, which is essential to mGluR1 function in SNpc dopaminergic neurons. In order to clarify the mechanisms by which NRG1 increases mGluR1 expression, we examined whether NRG1 activates PI3K-Akt-mTOR pathway in midbrain slices at different time points of incubation with NRG1 ( $5 \text{ nM}$  for 5, 15 and 30 min). We found that 5 min after NRG1 application the phosphorylation level of ErbB4 (Tyr1284) was increased when compared with control slices. The activation of ErbB4 receptor was followed by a

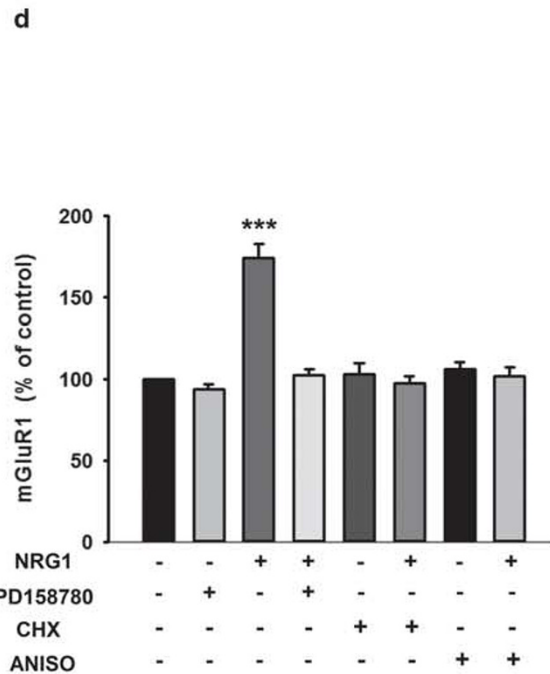
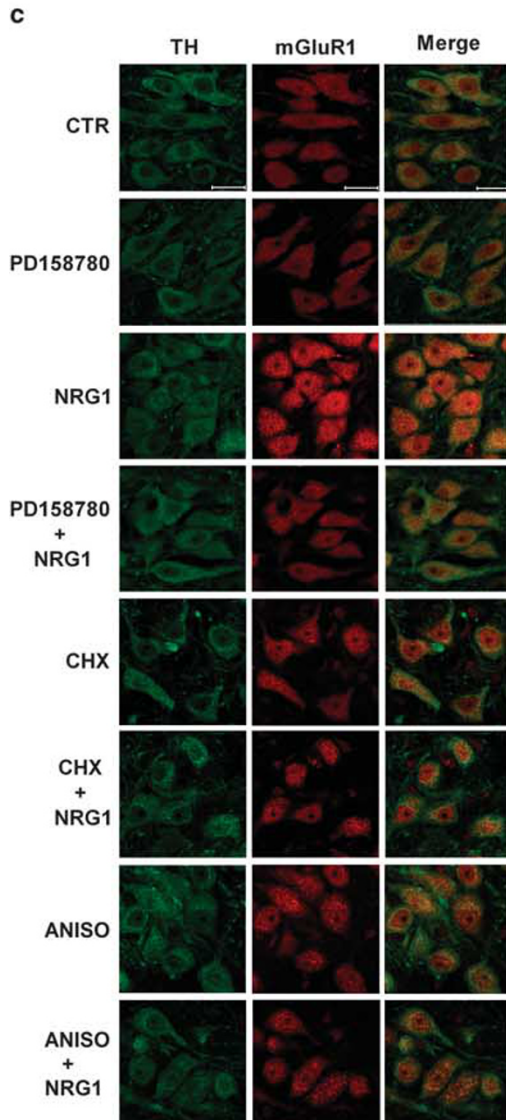
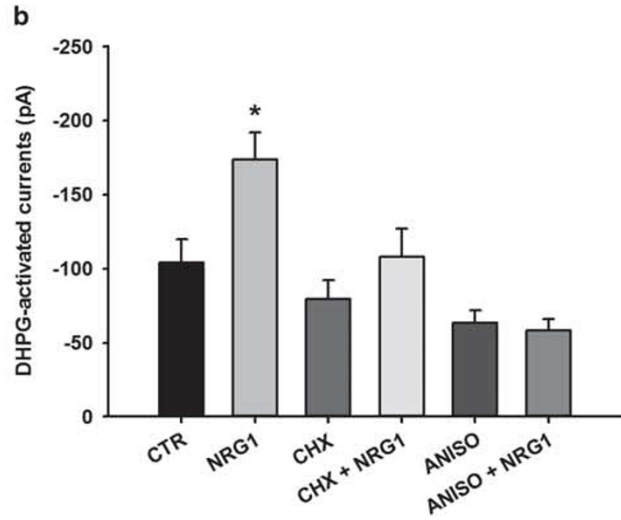
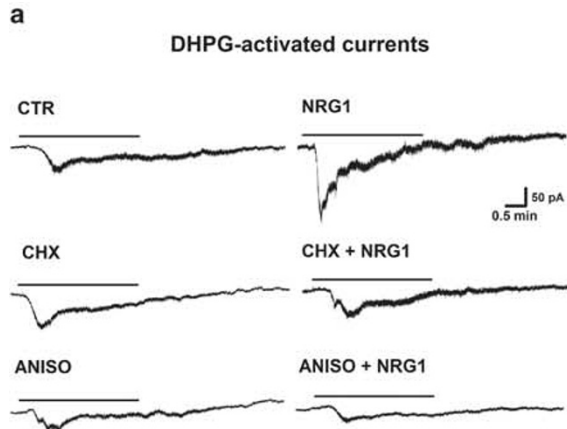
time-dependent increase of Akt and mTOR phosphorylation (Ser473 and Ser2448, respectively).

The activation of Akt-mTOR pathway 15 min after NRG1 application was associated with an increase of eEF2 expression together with a significant increase of mGluR1 protein levels (Figures 5a and b). Conversely, the expression levels of mGluR5, AMPAR subunit GluA1 and NMDAR subunit GluN2B were not significantly modified by NRG1 treatment (Figures 5a and b). These data indicate that exogenous application of NRG1 activates PI3K-Akt-mTOR pathway and induces a selective increase of mGluR1 expression in midbrain slices.

The depressant effect produced by ErbB inhibition on mGluR1 function may result from the inactivation of an intracellular pathway activated by endogenous NRG1 and essential for mGluR1 function. As NRG1 activates PI3K-Akt-mTOR pathway and ErbB receptors seem to interact directly with PI3K, it is possible that the binding of ErbB inhibitors is able to disrupt ErbB-PI3K interaction,

thus producing a quenching of NRG1-activated PI3K-Akt-mTOR pathway. In this case, the inhibition of PI3K-Akt-mTOR pathway at different points should mimic the depressant effect induced by ErbB inhibitors on mGluR1-activated responses.

To investigate this hypothesis, we evaluated the effects of two different PI3K inhibitors, LY294002 and wortmannin, on the mGluR1-activated currents. In the presence of both PI3K inhibitors (S)-DHPG-activated currents were significantly reduced. In





particular, bath application of LY294002 (25  $\mu\text{M}$ ) diminished these currents to  $28.16 \pm 2.30\%$  of control ( $n=5$ ,  $P < 0.001$ , paired *t*-test; Figure 5c). Similarly, superfusion of wortmannin (1  $\mu\text{M}$ ) induced a significant reduction of mGluR1-activated currents to  $34.58 \pm 10.65\%$  of control ( $n=5$ ,  $P < 0.01$ , paired *t*-test) (Figure 5d). We also tested whether inhibition of mTOR could mimic the depressant effect on mGluR1 function produced by ErbB inhibitors. The (S)-DHPG-activated currents were significantly reduced to  $30.48 \pm 9.36\%$  of control ( $n=5$ ,  $P < 0.01$ , paired *t*-test) in the presence of the mTOR inhibitor, rapamycin (1  $\mu\text{M}$ ; Figure 5e).

Collectively, these findings suggest that NRG1 activates ErbB receptor and the downstream PI3K-Akt-mTOR pathway; thus the inhibition of this pathway mimics the depressant effect induced by ErbB inhibitors on mGluR1-activated currents in SNpc dopaminergic neurons.

#### NRG1/ErbB signalling modulates mGluR1 trafficking

In order to investigate the effect of NRG1/ErbB signalling on mGluR1 trafficking, we monitored mGluR1 surface expression by biotinylation assay in midbrain slices treated with NRG1 (5 nM, 30 min) or PD158780 (10  $\mu\text{M}$ , 15 min). We found that the surface levels of mGluR1 were significantly reduced upon PD158780 treatment, whereas an increased mGluR1 surface expression was observed in NRG1-treated slices compared with control slices (Figures 6a and b). In line with the electrophysiological results (Figure 3), no changes were observed in NMDA receptor subunit GluN2B and in AMPA receptor subunit GluA1 (Figures 6a and b), thus excluding an effect of NRG1 and ErbB inhibition on glutamatergic ionotropic transmission.

To demonstrate that the reduction of mGluR1-dependent electrophysiological responses caused by ErbB inhibition in dopaminergic neurons is dependent on mGluR1 internalization, we investigated whether the depressant effect induced by the ErbB2 inhibitor AG879 could be counteracted by an inhibition of receptor endocytosis. Thus we evaluated the effect of AG879 on mGluR1-activated currents in the presence of dynasore, an inhibitor of clathrin/dynamin-dependent endocytosis. We observed a significant reduction of AG879-induced depression (Figures 6c and d). In particular, (S)-DHPG-activated currents were reduced to  $64.58 \pm 8.48\%$  of control by AG879 (10  $\mu\text{M}$ ) in the presence of dynasore (80  $\mu\text{M}$ ) while AG879 (10  $\mu\text{M}$ ) alone reduced mGluR1-activated currents to  $9.19 \pm 2.73\%$  of control ( $n=6$  each group,  $P < 0.001$ , AG879 vs AG879+dynasore, unpaired *t*-test). Bath application of dynasore (80  $\mu\text{M}$ ) *per se* did not significantly modify (S)-DHPG-activated currents (Figure 6d).

Altogether, these results demonstrate that NRG1/ErbB signalling bidirectionally regulates mGluR1 trafficking and that the functional inactivation of mGluR1 induced by ErbB inhibition is dependent on mGluR1 internalization.

NRG1/ErbB signalling modulates mGluR1-induced DA release in the striatum

NRG1/ErbB signalling could affect the function of mGluR1 in *in vivo* conditions, thus we performed microdialysis experiments in rats, to analyze whether the striatal DA release induced by intranigral injection of (S)-DHPG is modulated by blocking the endogenous NRG1/ErbB tone using the ErbB inhibitor PD158780 (Figure 7a). Statistical analyses revealed a significant treatment  $\times$  time interaction for DA in the rat striatum ( $F(18,126) = 4.027$ ;  $P < 0.001$ ). Intra-SNpc injection of (S)-DHPG (5 mM) produced a significant increase of DA level in the ipsilateral striatum ( $n=6$ ;  $F(9,50) = 2.147$ ;  $P < 0.05$ ), which was dependent on the activation of mGluR1 receptors, as it was completely blocked by an intra-SNpc pretreatment with the selective mGluR1 antagonist CPCOEt (10 mM). (Figures 7a and b). Notably, intra-SNpc injection of PD158780 (10  $\mu\text{M}$ ) applied 30 min before and then co-injected with (S)-DHPG in SNpc blocked striatal DA outflow induced by the application of (S)-DHPG in SNpc (Figure 7b). The baseline levels of DA for each group did not differ significantly from vehicle (DA in the striatum =  $1.598 \pm 0.22$  pg per 10  $\mu\text{l}$ ;  $F(5,26) = 0.400$ ;  $P > 0.05$ ). Moreover, striatal DA outflow in the groups treated with the intra-SNpc ErbB inhibitor or the mGluR1 antagonist did not change significantly from that treated with vehicle ( $F(18,108) = 0.816$ ;  $P > 0.05$ ;  $n=5$  for group).

These results confirm the essential role of endogenous nigral ErbB activation in the modulation of mGluR1-induced DA release in the striatum.

#### DISCUSSION

In this study, we have identified a novel functional interaction between NRG1/ErbB signalling and mGluR1 receptors in SNpc dopaminergic neurons that modulates the strength of striatal DA release. In particular, we have demonstrated that: (a) NRG1 selectively increases mGluR1-activated inward currents by inducing synthesis and trafficking to membrane of functional receptors; (b) NRG1 stimulates PI3K-Akt-mTOR pathway, whose activation is required for mGluR1 function; (c) a NRG1 endogenous tone sustains mGluR1 function, by maintaining the membrane surface expression of glutamate metabotropic receptors, and (d) NRG1/ErbB receptors and mGluR1 located on SNpc dopaminergic neurons regulates striatal DA release *in vivo*.

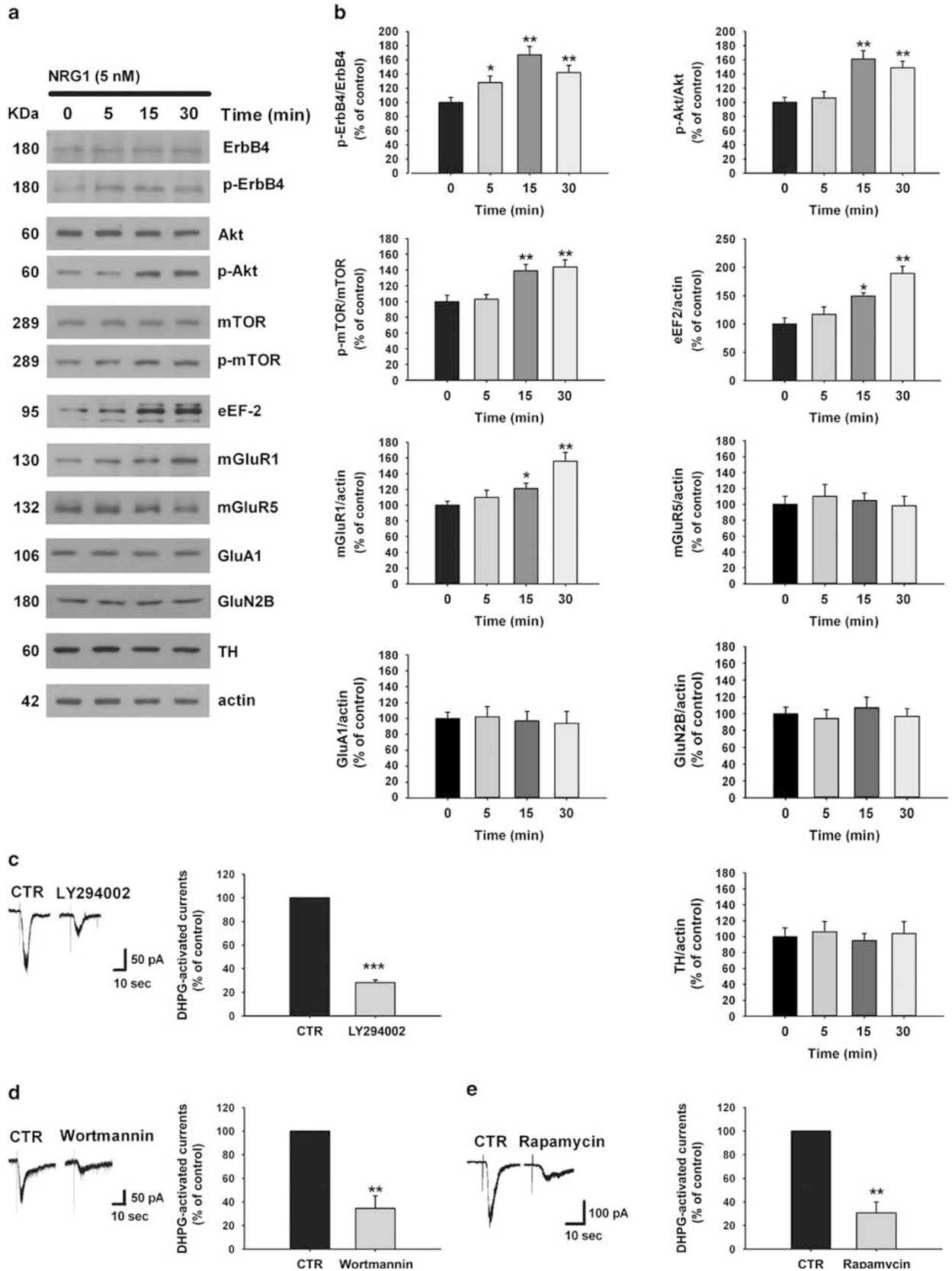
Although the expression of both NRG1 and ErbB receptors subunits (ErbB1–4) in mesencephalic dopaminergic neurons of rodent and human brain has been clearly demonstrated,<sup>6–9</sup> the function of ErbB signalling in this brain area has not been elucidated yet. Our results identify, for the first time, a functional role of NRG1/ErbB signalling in dopaminergic mesencephalic neurons, which control the activity of the nigrostriatal dopaminergic pathway.

Consolidated literature supports a role of NRG1/ErbB signalling in modulating the expression and/or function of ionotropic

**Figure 4.** Neuregulin 1 (NRG1) increases metabotropic glutamate receptor 1 (mGluR1) expression. (a) Representative traces of inward currents induced by bath application of (S)-3,5-dihydroxyphenylglycine ((S)-DHPG) (10  $\mu\text{M}$ , 3 min) in substantia nigra pars compacta dopaminergic neurons in control and in slices treated with: NRG1 (5 nM, 30 min), cycloheximide (CHX) (100  $\mu\text{M}$ , 60 min), CHX+NRG1 (CHX 100  $\mu\text{M}$ , 30 min prior to CHX 100  $\mu\text{M}$  plus NRG1 5 nM, 30 min), anisomycin (ANISO) (40  $\mu\text{M}$ , 60 min) and ANISO+NRG1 (anisomycin 40  $\mu\text{M}$ , 30 min prior to anisomycin 40  $\mu\text{M}$  plus NRG1 5 nM, 30 min). (b) Mean amplitudes of (S)-DHPG-activated currents (pA) in the indicated pharmacological conditions: CTR ( $n=17$ ), NRG1 ( $n=13$ ), CHX ( $n=11$ ), CHX+NRG1 ( $n=11$ ), ANISO ( $n=10$ ), ANISO+NRG1 ( $n=10$ ); \* $P < 0.05$ , one-way analysis of variance (ANOVA) followed by Holm–Sidak test. (c) Double-labelled confocal images of TH (green) and mGluR1 (red) in control condition (CTR) and upon treatments with NRG1 (5 nM, 30 min), PD158780 (10  $\mu\text{M}$ , 15 min), PD158780 +NRG1 (NRG1 5 nM, 30 min preceded by PD158780 10  $\mu\text{M}$ , 15 min), CHX (100  $\mu\text{M}$ , 60 min), CHX+NRG1 (CHX 100  $\mu\text{M}$ , 30 min prior to CHX 100  $\mu\text{M}$  plus NRG1 5 nM, 30 min), ANISO (40  $\mu\text{M}$ , 60 min), ANISO +NRG1 (anisomycin 40  $\mu\text{M}$ , 30 min prior to anisomycin 40  $\mu\text{M}$  plus NRG1 5 nM, 30 min). Scale bar 20  $\mu\text{m}$ . (d) Histograms of densitometric values of mGluR1 levels, following the indicated treatments, expressed as mean fluorescence of individual TH-positive cells, normalized to total cellular surface. Data are expressed as mean  $\pm$  s.d. (control is indicated as 100%). One-way ANOVA followed by Bonferroni's multiple comparison test. \*\*\* $P < 0.001$  (200 cells/group;  $n=3$ ).

receptors, such as NMDARs, AMPARs, nicotinic acetylcholine receptors and GABA<sub>A</sub>Rs<sup>32–39</sup> and ion channels.<sup>56–58</sup> Regarding a functional interaction between NRG1 and metabotropic glutamate receptors, Schapansky *et al.*<sup>40</sup> have reported that a prolonged

(24 h) treatment with NRG1 modulates the changes of intracellular calcium levels caused by a broad spectrum (group I/II) mGluRs agonist in rat hippocampal cultures. Thus our results identify a yet uncharacterized role of NRG1/ErbB signalling as key regulator of



the functional expression of a specific G protein-coupled metabotropic glutamate receptor in native mesencephalic dopaminergic neurons recorded *in vitro*.

As (S)-DHPG is an agonist for group I mGluRs activating both mGluR1 and mGluR5,<sup>54</sup> the NRG1-induced increase of the (S)-DHPG-activated currents might involve both receptors. However, the observation that the effect of NRG1 on the (S)-DHPG-activated currents is completely abolished in the presence of the selective mGluR1 antagonist, CPCCOEt, and remains unaffected in the presence of the specific mGluR5 antagonist, MPEP, demonstrates that the potentiation of the (S)-DHPG-induced responses caused by NRG1 is purely

dependent on a mGluR1 activation. Accordingly, the NRG1 treatment caused a significant increase in the levels of mGluR1 protein in midbrain slices without modifying the expression of mGluR5.

The NRG1-induced effects depended on the activation of ErbB receptors, as demonstrated by data showing that both the potentiation of (S)-DHPG-activated currents and the increase in mGluR1 immunoreactivity were antagonized by a treatment with the ErbB inhibitor PD158780.

Interestingly, our results also support a tonic role of endogenous NRG1 in sustaining mGluR1 function in SNpc DAergic neurons as either diminishing ErbB signalling, by means of a broad

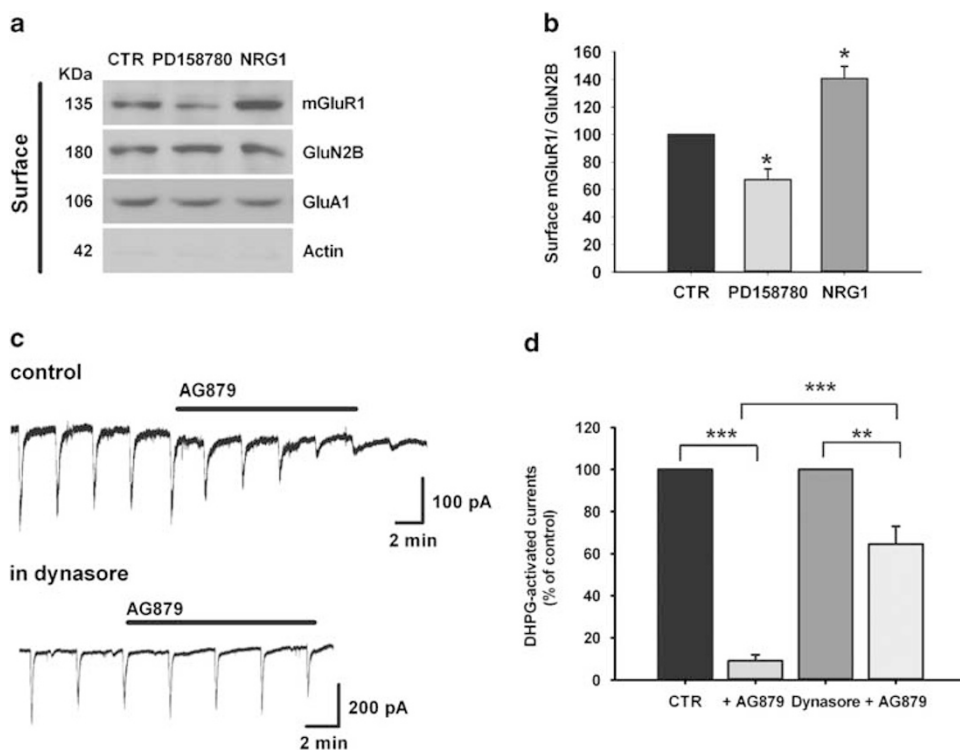


**Figure 6.** ErbB inhibition induces internalization of metabotropic glutamate receptor 1 (mGluR1). **(a)** Representative immunoblot of surface mGluR1, GluN2B and GluA1 determined by biotinylation assay. Substantia nigra pars compacta was isolated from midbrain slices after incubation with vehicle (CTR), PD158780 (10  $\mu$ M; 15 min) or NRG1 (5 nM; 30 min). Absence of actin in surface samples indicates specificity of the biotinylation assay. **(b)** Densitometric quantification of changes in gray values are expressed as mean  $\pm$  s.d. (control is indicated as 100%), and the level of mGluR1 is normalized with respect to the level of GluN2B. One-way analysis of variance followed by Bonferroni's multiple comparison test. \* $P < 0.05$  ( $n = 3$ ). **(c)** Representative traces showing the effect of bath applied AG879 (10  $\mu$ M) on inward current induced by pressure application of (S)-3,5-dihydroxyphenylglycine ((S)-DHPG) (100  $\mu$ M, 1.5–2.5 s) in control condition (left) and in the presence of dynasore (80  $\mu$ M) (right). **(d)** Histogram of (S)-DHPG-activated current mean amplitudes (percentage of control) showing that in the presence of dynasore the inhibitory effect of AG879 is significantly reduced ( $n = 6$  each group,  $P < 0.001$ , unpaired *t*-test).

**Figure 5.** Neuregulin 1 (NRG1) activates phosphatidylinositol 3-kinase-Akt-mammalian target of rapamycin (PI3K-Akt-mTOR) pathway, which is essential to metabotropic glutamate receptor 1 (mGluR1) function in substantia nigra pars compacta (SNpc) dopaminergic neurons. **(a and b)** NRG1 application activates Akt-mTOR pathway and increases mGluR1 expression in SNpc. **(a)** Representative immunoblots of protein extracted from SNpc isolated from midbrain slices after incubation with NRG1 (5 nM) for 5, 15 and 30 min and probed with the indicated antibodies. **(b)** Densitometric quantification of changes in gray values of the indicated protein expressed as mean  $\pm$  s.d. (percentage of control). The relative fold change in the levels of phosphorylated proteins (p-ErbB4, p-Akt, p-mTOR) was normalized with respect to the total protein levels (ErbB4, Akt, mTOR, respectively). The levels of eEF2, mGluR1, mGluR5, GluA1, GluN2B and TH were normalized with respect to the level of actin, used as loading control ( $n = 3$ , \*\*\* $P < 0.01$ , \* $P < 0.05$ , one-way analysis of variance with a Bonferroni's *post-hoc* test). **(c–e)** Inactivation of PI3K-Akt-mTOR pathway reduces mGluR1-activated currents. **(c)** Representative traces (left) and mean current amplitudes, (percentage of control) (right) activated by pressure application of (S)-3,5-dihydroxyphenylglycine ((S)-DHPG) (100  $\mu$ M, 2 s) before and during bath application of the PI3K inhibitor, LY294002 (25  $\mu$ M, 30 min) ( $n = 5$ , \*\*\* $P < 0.001$ , paired *t*-test). **(d)** Representative traces (left) and mean current amplitudes (percentage of control) (right), induced by pressure application of (S)-DHPG (100  $\mu$ M, 1.5 s) before and during treatment with the PI3K inhibitor, wortmannin (1  $\mu$ M, 30 min) ( $n = 5$ , \*\*\* $P < 0.01$ , paired *t*-test). **(e)** Representative traces (left) and mean current amplitudes (percentage of control, right) induced by pressure application of (S)-DHPG (100  $\mu$ M, 2 s) before and during treatment with the mTOR inhibitor, rapamycin (1  $\mu$ M, 30 min) ( $n = 5$ , \*\*\* $P < 0.01$ , paired *t*-test).

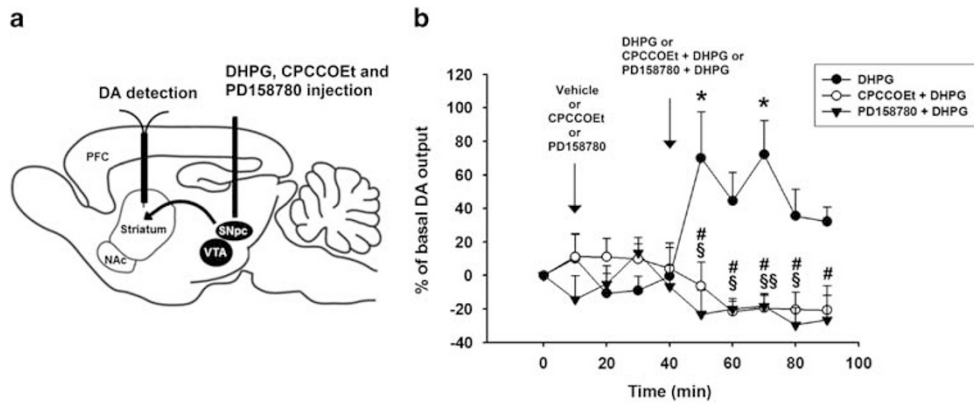


**Figure 7.** Striatal dopamine release *in vivo* is modulated by the metabotropic glutamate receptor 1/Neuregulin 1/ErbB signalling in the substantia nigra pars compacta. **(a)** Schematic representation of the experimental protocol used in microdialysis experiments performed in awake, freely moving rats to investigate the effect of intra-nigral injection of CPCCOEt or PD158780 on dopamine outflow in the striatum induced by intra-nigral injection of 3,5-dihydroxyphenylglycine (DHPG). **(b)** Striatal dopamine levels expressed as percentage of changes (means  $\pm$  s.e.) from basal values. Rats were divided in three groups: rats receiving a first injection of vehicle followed, after 30 min, by the injection of DHPG (5 mM) ( $n=6$ ), rats receiving a first injection of CPCCOEt (10 mM) followed, after 30 min, by the injection of CPCCOEt (10 mM) plus DHPG (5 mM) ( $n=5$ ), and rats receiving a first injection of PD158780 (10  $\mu$ M) followed, after 30 min, by the injection of PD158780 (10  $\mu$ M) plus DHPG (5 mM) ( $n=6$ ). Statistical analyses were performed on raw data. \* $P < 0.05$ , from the basal values, repeated-measures analysis of variance (ANOVA);  $^{\#}P < 0.05$ ,  $^{\#\#}P < 0.01$ , one-way ANOVA, DHPG vs CPCCOEt+DHPG at each time point;  $^{*}P < 0.01$  one-way ANOVA, DHPG vs PD158780+DHPG at each time point.

spectrum antagonist, or interfering with NRG1 maturation, by inhibiting the metalloproteases enzymes, leads to a reduction of mGluR1-activated currents. Moreover, the evidence that the mGluR1-activated currents are reduced in the presence of AG879, a selective ErbB2 inhibitor, together with the result showing that NRG1 is able to induce ErbB4 phosphorylation and activation, restricts to the heterodimers ErbB2/ErbB4, ErbB2/ErbB3 or homodimer ErbB4/ErbB4 the possible subunit compositions of the ErbB receptors mediating the NRG1 effects.

Of note, the effect of NRG1/ErbB signalling on glutamatergic transmission in SNpc DAergic neurons appears to be highly specific for the mGluR1-activated responses, because ionotropic NMDAR- and AMPAR-activated currents were not affected. Our data on glutamate ionotropic receptors are in strict compliance with other works showing the different effects of NRG1 in various brain areas and synapses, reporting potentiation, reduction or no effect on the expression and/or function of AMPARs and NMDARs. For instance, a NRG1-induced modulatory effect on NMDARs expression and/or function has been detected in the prefrontal cortex<sup>37</sup> and in the cerebellum<sup>34</sup> but not in the hippocampus<sup>32</sup> while functional expression of AMPARs is differently influenced by NRG1 in the hippocampus<sup>32</sup> and in the prefrontal cortex.<sup>38</sup> Moreover, in accordance with a specific action, the evidence that the muscarine-activated currents are not affected by NRG1 suggests that, at least in SNpc DAergic neurons, NRG1/ErbB signalling does not modulate other metabotropic receptors linked to Gq proteins and coupled to TRPCs.

The increase of mGluR1-activated currents induced by NRG1 is due to the exposure at membrane sites of newly synthesized functional receptors, through the activation of PI3K-Akt-mTOR pathway. In fact, the increase of both mGluR1 staining and (S)-DHPG-activated currents, induced by NRG1, are blocked by two different protein synthesis inhibitors, CHX and ANISO. Additionally, our results from biotinylation assay confirm an enhancement of mGluR1 membrane expression after NRG1 treatment. Several reports demonstrate that NRG1 induces activation of PI3K-Akt-mTOR pathway, thus modulating the expression of different receptors and ion channels.<sup>33,56–58</sup> Accordingly, we found that NRG1 induces the activation of PI3K-Akt-mTOR in midbrain slices together with an increased expression of eEF2, which is involved

in translation phases of protein synthesis, and enhanced levels of mGluR1 protein. Moreover, the pharmacological inactivation of PI3K-Akt-mTOR pathway, at different points, produces a reduction of (S)-DHPG-activated currents, thus mimicking the depressant effect on mGluR1 function induced by ErbB inhibitors.

Internalization of receptors into cytoplasm is a common mechanism of attenuation of GPCR-activated signalling.<sup>59</sup> Similarly to other GPCRs, mGluR1 internalization is mediated by a mechanism that involves the formation of endocytotic clathrin-coated vesicles, dependent on dynamin action.<sup>60,61</sup> Our results demonstrate that functional inhibition of mGluR1 induced by blocking NRG1 signalling is due to the internalization of receptors. Indeed, by means of biotinylation assay, we show that ErbB inhibitors reduced mGluR1 membrane expression, and the reduction of mGluR1-activated currents is counteracted by blocking dynamin-dependent GPCR endocytosis with dynasore. As mGluR1 have a high rate of constitutive internalization that is independent of agonist stimulation,<sup>62</sup> a net reduction in mGluR1 membrane expression could occur as consequence of a block of a tonic recycling process. Therefore, the reduction of functional expression of mGluR1 induced by blocking endogenous ErbB signalling might be due to an interference in the here reported mechanism of new synthesis and trafficking to membrane of mGluR1 induced by NRG1. Moreover, as both ErbB receptor and mGluR1 are localized in the PSD of excitatory synapses, there is the possibility that they could physically interact, directly or through scaffolding proteins like PSD-95 and the GKAP-Shank-Homer complex.<sup>4</sup> In this context, ErbB inhibition by producing a conformational modification might disrupt ErbB-mGluR1 interaction, thus inducing mGluR1 internalization.

#### Physiological and pathological implications

As mGluR1 is critically involved in neurodevelopment, in synaptic plasticity and in different neuropsychiatric and neurodegenerative disorders,<sup>45,48,49</sup> mechanisms regulating its functional expression such as the ones dependent on NRG1 might be relevant in several physiological and pathological conditions being crucial for the amount of DA released in the striatum and other projecting areas.

In relation to the *in vivo* physiological relevance of mGluR1 located on SNpc dopaminergic neurons, here we report that the activation of these receptors by the intranigral microinjection of DHPG induces DA efflux in striatal projection areas. Interestingly, this effect is blocked by the local application of a specific mGluR1 antagonist. Accordingly, it has been previously reported that an intra-ventral tegmental area DHPG injection induces a rise of extracellular DA in medial prefrontal cortex, which is mainly mediated by the activation of somatodendritic mGluR1 located on dopaminergic neurons.<sup>44</sup> The increase in striatal DA efflux caused by the injection of DHPG into the rat SNpc is consistent with the depolarizing effects of this mGluR1 agonist on the dopaminergic cells maintained *in vitro*,<sup>41</sup> and might have a role in the control of locomotor activation, motivation and cognition.<sup>63,64</sup> In support of the role of mGluR1 in modulating the function of the dopaminergic system, it has been reported that microinjection of DHPG in the ventral tegmental area and nucleus accumbens causes an increase in locomotor activity in rodents<sup>65</sup> and that a pharmacological inhibition of mGluR1 impairs motor learning.<sup>66</sup> Remarkably, in the present study, we have shown that the DHPG-induced DA release in the striatum is prevented by the local (SNpc) administration of the ErbB inhibitor, PD158780. These *in vivo* results are in line with the *in vitro* experiments, demonstrating for the first time the essential role of NRG1 receptors in the modulation of glutamate metabotropic receptors-dependent responses in the dopaminergic system of a living animal.

Interestingly, *NRG1* is considered an important susceptibility gene for schizophrenia.<sup>4</sup> However, the exact mechanism by which an alteration of NRG1 signalling leads to this disease remains to be clarified. As one of the cardinal pathological features of schizophrenia is perturbation of synaptic connectivity,<sup>67</sup> the evidence that NRG1 can differently regulate the expression and the function of several ionotropic receptors supports the hypothesis that dysregulation of NRG1/ErbB signalling could result in altered synaptic function and information processing.<sup>4,67</sup> It has to be considered that both disturbances in dopaminergic and glutamatergic transmission have been implicated in the pathological mechanisms of schizophrenia.<sup>67,68</sup> To this regard, recent evidence supports a specific role of SNpc dopaminergic neurons in this pathology.<sup>69–74</sup>

Interestingly, besides ionotropic NMDARs, a role for mGluR1 in this disease has been recently hypothesized.<sup>75</sup> For instance, the expression profile of mGluR1 in brain areas crucially involved in schizophrenia such as the cortex, the hippocampus and the dopaminergic mesencephalic nuclei<sup>76–78</sup> suggests their involvement in this devastating disease. Remarkably, different mutations in *mGluR1* gene<sup>79</sup> and alterations in the expression levels and signalling of mGluR1<sup>80,81</sup> have been reported in schizophrenic patients. Moreover, deficits in sensorimotor gating similar to those seen in schizophrenia have been observed in mice knockout for mGluR1.<sup>82</sup> In light of the modulatory role of NRG1 described in this study, it might be possible that a dysregulation in mGluR1 function in schizophrenia could be eventually secondary to NRG1 alterations. Furthermore, as recent evidence indicate that the hyperactivation of SNpc DAergic neurons contributes to the pathological alteration observed in schizophrenic patients,<sup>71–74</sup> our results, identifying a novel mechanism by which NRG1 regulates the activity of dopaminergic neurons via mGluR1, suggest NRG1 as a possible dysfunctional link between glutamate and DA in the complex picture of schizophrenia.

Interestingly, it has been recently reported that either in neurotoxin-induced models of PD or in the brain of Parkinsonian patients there is a downregulation of TRPC channels associated with an inactivation of PI3K-Akt-mTOR pathway.<sup>83</sup> Moreover, NRG1/ErbB signalling displays a neurotrophic and neuroprotective role in dopaminergic neurons in primary cultures<sup>26</sup> and in a PD animal model.<sup>27</sup> Therefore, it might be possible that the enhancement/maintenance of mGluR1/TRPC transmission

regulated by NRG1 reported here could contribute to the trophic state of SNpc dopaminergic neurons and be critically involved in PD pathogenetic mechanisms.

In conclusion, our results unveil an essential role of NRG1/ErbB tone in sustaining mGluR1 function, thus modulating the functional state of the dopaminergic system and consequently the release of DA in the terminal areas. This NRG1-mediated mechanism might have important implications in physiological functions, such as movement, motivation and cognition. On the other hand, in case of deregulated NRG1-mGluR1 function in the dopaminergic neurons, brain diseases such as Parkinson's disease and schizophrenia could eventually occur.

## CONFLICT OF INTEREST

The authors declare no conflict of interest.

## ACKNOWLEDGMENTS

This work has been financed by Grants from the Minister of Health to NBM, Alzheimer's Association (NIRG-11-204588) to MDA and the Italian Ministry of University and Research (PRIN 2009) to MDA.

## REFERENCES

- Burden S, Yarden Y. Neuregulins and their receptors: a versatile signaling module in organogenesis and oncogenesis. *Neuron* 1997; **18**: 847–855.
- Buonanno A, Fischbach GD. Neuregulin and ErbB receptor signaling pathways in the nervous system. *Curr Opin Neurobiol* 2001; **11**: 287–296.
- Falls DL. Neuregulins: functions, forms, and signalling strategies. *Exp. Cell Res* 2003; **284**: 14–30.
- Mei L, Xiong WC. Neuregulin 1 in neural development, synaptic plasticity and schizophrenia. *Nat Rev Neurosci* 2008; **9**: 437–452.
- Iwakura Y, Nawa H. ErbB1-4 dependent EGF/neuregulin signals and their crosstalk in the central nervous system: pathological implications in schizophrenia and Parkinson's disease. *Front Cell Neurosci* 2013; **7**: 1–13.
- Steiner H, Blum M, Kitai ST, Fedi P. Differential expression of ErbB3 and ErbB4 neuregulin receptors in dopamine neurons and forebrain areas of the adult rat. *Exp Neurol* 1999; **159**: 494–503.
- Kerber G, Streif R, Schwaiger FW, Kreutzberg GW, Hager G. Neuregulin-1 isoforms are differentially expressed in the intact and regenerating adult rat nervous system. *J Mol Neurosci* 2003; **21**: 149–165.
- Law AJ, Shannon Weickert C, Hyde TM, Kleinman JE, Harrison PJ. Neuregulin-1 (NRG-1) mRNA and protein in the adult human brain. *Neuroscience* 2004; **127**: 125–136.
- Abe Y, Namba H, Zheng Y, Nawa H. In situ hybridization reveals developmental regulation of ErbB1-4 mRNA expression in mouse midbrain: implication of ErbB receptors for dopaminergic neurons. *Neuroscience* 2009; **161**: 95–110.
- Stefansson H, Sigurdsson E, Steinthorsdottir V, Bjornsdottir S, Sigmundsson T, Ghosh S *et al*. Neuregulin 1 and susceptibility to schizophrenia. *Am J Hum Genet* 2002; **71**: 877–892.
- Yang JZ, Si TM, Ruan Y, Ling YS, Han YH, Wang XL *et al*. Association study of neuregulin 1 gene with schizophrenia. *Mol Psychiatry* 2003; **8**: 706–709.
- Munafò MR, Thielson DL, Clark TG, Flint J. Association of the NRG1 gene and schizophrenia: a meta-analysis. *Mol Psychiatry* 2006; **11**: 539–546.
- Shi J, Levinson DF, Duan J, Sanders AR, Zheng Y, Pe'er I *et al*. Common variants on chromosome 6p22.1 are associated with schizophrenia. *Nature* 2009; **460**: 753–757.
- Hashimoto R, Straub RE, Weickert CS, Hyde TM, Kleinman JE, Weinberger DR. Expression analysis of neuregulin-1 in the dorsolateral prefrontal cortex in schizophrenia. *Mol Psychiatry* 2004; **9**: 299–307.
- Petryshen TL, Middleton FA, Kirby A, Aldinger KA, Purcell S, Tahl AR *et al*. Support for involvement of neuregulin 1 in schizophrenia pathophysiology. *Mol Psychiatry* 2005; **10**: 366–374.
- Law AJ, Lipska BK, Weickert CS, Hyde TM, Straub RE, Hashimoto R *et al*. Neuregulin 1 transcripts are differentially expressed in schizophrenia and regulated by 5' SNPs associated with the disease. *Proc Natl Acad Sci USA* 2006; **103**: 6747–6752.
- Hahn CG, Wang HY, Cho DS, Talbot K, Gur RE, Berrettini WH *et al*. Altered neuregulin 1-erbB4 signaling contributes to NMDA receptor hypofunction in schizophrenia. *Nat Med* 2006; **12**: 824–828.
- du Bois TM, Newell KA, Huang XF. Perinatal phencyclidine treatment alters neuregulin 1/erbB4 expression and activation in later life. *Eur Neuropsychopharmacol* 2012; **22**: 356–363.

- 19 Radonjić NV, Jakovcević I, Bumbaširević V, Petronijević ND. Perinatal phencyclidine administration decreases the density of cortical interneurons and increases the expression of neuregulin-1. *Psychopharmacology* 2013; **227**: 673–683.
- 20 Gerlai R, Pisacane P, Erickson S. Heregulin, but not ErbB2 or ErbB3, heterozygous mutant mice exhibit hyperactivity in multiple behavioral tasks. *Behav Brain Res* 2000; **109**: 219–227.
- 21 Golub MS, Germann SL, Lloyd KC. Behavioral characteristics of a nervous system-specific erbB4 knock-out mouse. *Behav Brain Res* 2004; **153**: 159–170.
- 22 Deakin IH, Law AJ, Oliver PL, Schwab MH, Nave KA, Harrison PJ, Bannerman DM. Behavioural characterization of neuregulin 1 type I overexpressing transgenic mice. *Neuroreport* 2009; **20**: 1523–1528.
- 23 Deakin IH, Nissen W, Law AJ, Lane T, Kanso R, Schwab MH *et al*. Transgenic overexpression of the type I isoform of neuregulin 1 affects working memory and hippocampal oscillations but not long-term potentiation. *Cereb Cortex* 2012; **22**: 1520–1529.
- 24 Kato T, Kasai A, Mizuno M, Fengyi L, Shintani N, Maeda S *et al*. Phenotypic characterization of transgenic mice overexpressing neuregulin-1. *PLoS One* 2010; **5**: 1–13.
- 25 Yin DM, Chen YJ, Lu YS, Bean JC, Sathyamurthy A, Shen C *et al*. Reversal of behavioral deficits and synaptic dysfunction in mice overexpressing neuregulin 1. *Neuron* 2013; **78**: 644–657.
- 26 Zhang L, Fletcher-Turner A, Marchionni MA, Apparsundaram S, Lundgren KH, Yurek DM *et al*. Neurotrophic and neuroprotective effects of the neuregulin glial growth factor-2 on dopaminergic neurons in rat primary midbrain cultures. *J Neurochem* 2004; **91**: 1358–1368.
- 27 Carlsson T, Schindler FR, Höllerhage M, Depboylu C, Arias-Carrión O, Schnurrbusch S *et al*. Systemic administration of neuregulin-1 $\beta$ 1 protects dopaminergic neurons in a mouse model of Parkinson's disease. *J Neurochem* 2011; **117**: 1066–1074.
- 28 Depboylu C, Höllerhage M, Schnurrbusch S, Brundin P, Oertel WH, Schratzenholz A *et al*. Neuregulin-1 receptor tyrosine kinase ErbB4 is upregulated in midbrain dopaminergic neurons in Parkinson disease. *Neurosci Lett* 2012; **531**: 209–214.
- 29 Kato T, Abe Y, Sotoyama H, Kakita A, Kominami R, Hirokawa S *et al*. Transient exposure of neonatal mice to neuregulin-1 results in hyperdopaminergic states in adulthood: implication in neurodevelopmental hypothesis for schizophrenia. *Mol Psychiatry* 2011; **16**: 307–320.
- 30 Newell KA, Karl T, Huang XF. A neuregulin 1 transmembrane domain mutation causes imbalanced glutamatergic and dopaminergic receptor expression in mice. *Neuroscience* 2013; **248**: 670–680.
- 31 Yurek DM, Zhang L, Fletcher-Turner A, Seroogy KB. Supranigral injection of neuregulin1-beta induces striatal dopamine overflow. *Brain Res* 2004; **1028**: 116–119.
- 32 Kwon OB, Paredes D, Gonzalez CM, Neddens J, Hernandez L, Vullhorst D *et al*. Neuregulin-1 regulates LTP at CA1 hippocampal synapses through activation of dopamine D4 receptors. *Proc Natl Acad Sci USA* 2008; **105**: 15587–15592.
- 33 Tansey MG, Chu GC, Merlie JP. ARIA/HRG regulates AChR epsilon subunit gene expression at the neuromuscular synapse via activation of phosphatidylinositol 3-kinase and Ras/MAPK pathway. *J Cell Biol* 1996; **134**: 465–476.
- 34 Ozaki M, Sasner M, Yano R, Lu HS, Buonanno A. Neuregulin-beta induces expression of an NMDA-receptor subunit. *Nature* 1997; **390**: 691–694.
- 35 Rieff HI, Raetzman LT, Sapp DW, Yeh HH, Siegel RE, Corfas G. *et al*. Neuregulin induces GABAA receptor subunit expression and neurite outgrowth in cerebellar granule cells. *J Neurosci* 1999; **19**: 10757–10766.
- 36 Okada M, Corfas G. Neuregulin 1 downregulates postsynaptic GABAA receptors at the hippocampal inhibitory synapse. *Hippocampus* 2004; **14**: 337–344.
- 37 Gu Z, Jiang Q, Fu AKY, Ip NY, Yan Z. Regulation of NMDA receptors by neuregulin signaling in prefrontal cortex. *J Neurosci* 2005; **25**: 4974–4984.
- 38 Abe Y, Namba H, Kato T, Iwakura Y, Nawa H. Neuregulin-1 signals from the periphery regulate AMPA receptor sensitivity and expression in GABAergic interneurons in developing neocortex. *J Neurosci* 2011; **31**: 5699–5709.
- 39 Li B, Woo RS, Mei L, Malinow R. The neuregulin-1 receptor erbB4 controls glutamatergic synapse maturation and plasticity. *Neuron* 2007; **54**: 583–597.
- 40 Schapansky J, Morissette M, Odero G, Albensi B, Glazner G. Neuregulin beta1 enhances peak glutamate-induced intracellular calcium levels through endoplasmic reticulum calcium release in cultured hippocampal neurons. *Can J Physiol Pharmacol* 2009; **87**: 883–891.
- 41 Guatteo E, Mercuri NB, Bernardi G, Knöpfel T. Group I metabotropic glutamate receptors mediate an inward current in rat substantianigra dopamine neurons that is independent from calcium mobilization. *J Neurophysiol* 1999; **82**: 1974–1981.
- 42 Tozzi A, Bengtson CP, Longone P, Carignani C, Fusco FR, Bernardi G *et al*. Involvement of transient receptor potential-like channels in responses to mGluR1 activation in midbrain dopamine neurons. *Eur J Neurosci* 2003; **18**: 2133–2145.
- 43 Prisco S, Natoli S, Bernardi G, Mercuri NB. Group I metabotropic glutamate receptors activate burst firing in rat midbrain dopaminergic neurons. *Neuropharmacology* 2002; **42**: 289–296.
- 44 Renoldi G, Calcagno E, Borsini F, Invernizzi RW. Stimulation of group I mGlu receptors in the ventrotemporal area enhances extracellular dopamine in the rat medial prefrontal cortex. *J Neurochem* 2007; **100**: 1658–1666.
- 45 Catania MV, D'Antoni S, Bonaccorso CM, Aronica E, Bear MF, Nicoletti F *et al*. Group I metabotropic glutamate receptors: a role in neurodevelopmental disorders? *Mol Neurobiol* 2007; **35**: 298–307.
- 46 Aiba A, Kano M, Chen C, Stanton ME, Fox GD, Herrup K *et al*. Deficient cerebellar long-term depression and impaired motor learning in mGluR1 mutant mice. *Cell* 1994; **79**: 377–388.
- 47 Aiba A, Chen C, Herrup K, Rosenmund C, Stevens CF, Tonegawa S. (1994). Reduced hippocampal long-term potentiation and context-specific deficit in associative learning in mGluR1 mutant mice. *Cell* 1994; **79**: 365–375.
- 48 Lüscher C, Huber KM. Group 1 mGluR-dependent synaptic long-term depression (mGluR-LTD): mechanisms and implications for circuitry & disease. *Neuron* 2010; **65**: 445–459.
- 49 Ferraguti F, Crepaldi L, Nicoletti F. Metabotropic glutamate 1 receptor: current concepts and perspectives. *Pharmacol Rev* 2008; **60**: 536–581.
- 50 Mercuri NB, Bonci A, Calabresi P, Stefani A, Bernardi G. Properties of the hyperpolarization-activated cation current Ih in rat midbrain dopaminergic neurons. *Eur J Neurosci* 1995; **7**: 462–469.
- 51 Gladding CM, Collett VJ, Jia Z, Bashir ZI, Collingridge GL, Molnár E *et al*. Tyrosine dephosphorylation regulates AMPAR internalisation in mGluR-LTD. *Mol Cell Neurosci* 2009; **40**: 267–279.
- 52 Paxinos G, Watson C. *The Rat Brain in Stereotaxic Coordinates*, 5th edn. Academic Press, 2005.
- 53 Federici M, Latagliata EC, Ledonne A, Rizzo FR, Feligioni M, Sulzer D *et al*. Paradoxical abatement of striatal dopaminergic transmission by cocaine and methylphenidate. *J Biol Chem* 2014; **289**: 264–274.
- 54 Schoepp DD, Goldsworthy J, Johnson BG, Salhoff CR, Baker SR. 3,5-Dihydroxyphenylglycine is a highly selective agonist for phosphoinositide-linked metabotropic glutamate receptors in the rat hippocampus. *J Neurochem* 1994; **63**: 769–772.
- 55 Shimizu S, Wakamori M, Maeda A, Kurosaki T, Takada N *et al*. Molecular cloning and functional characterization of a novel receptor-activated TRP Ca<sup>2+</sup> channel from mouse brain. *J Biol Chem* 1998; **273**: 10279–10287.
- 56 Subramony P, Dryer SE. Neuregulins stimulate the functional expression of Ca<sup>2+</sup>-activated K<sup>+</sup> channels in developing chicken parasympathetic neurons. *Proc Natl Acad Sci USA* 1997; **94**: 5934–5938.
- 57 Canetta SE, Luca E, Pertot E, Role LW, Talmage DA. Type III Nrg1 back signaling enhances functional TRPV1 along sensory axons contributing to basal and inflammatory thermal pain sensation. *PLoS One* 2011; **6**: 1–16.
- 58 Yao JJ, Sun J, Zhao QR, Wang CY, Mei YA. Neuregulin-1/ErbB4 signaling regulates Kv4.2-mediated transient 2 outward K<sup>+</sup> current through the Akt/mTOR pathway. *Am J Physiol Cell Physiol* 2013; **305**: 197–206.
- 59 Magalhaes AC, Dunn H, Ferguson SS. Regulation of GPCR activity, trafficking and localization by GPCR-interacting proteins. *Br J Pharmacol* 2012; **165**: 1717–1736.
- 60 Mundell SJ, Matharu AL, Pula G, Roberts PJ, Kelly E. Agonist-induced internalization of the metabotropic glutamate receptor 1a is arrestin- and dynamin-dependent. *J Neurochem* 2001; **78**: 546–551.
- 61 Dhami GK, Ferguson SS. Regulation of metabotropic glutamate receptor signaling, desensitization and endocytosis. *Pharmacol Ther* 2006; **111**: 260–271.
- 62 Dale LB, Bhattacharya M, Seachrist JL, Anborgh PH, Ferguson SS. Agonist-stimulated and tonic internalization of metabotropic glutamate receptor 1a in human embryonic kidney 293 cells: agonist-stimulated endocytosis is beta-arrestin1 isoform-specific. *Mol Pharmacol* 2001; **60**: 1243–1253.
- 63 Cenci MA. Dopamine dysregulation of movement control in L-DOPA-induced dyskinesia. *Trends Neurosci* 2007; **30**: 236–243.
- 64 Simpson EH, Kellendonk C, Kandel E. A possible role for the striatum in the pathogenesis of the cognitive symptoms of schizophrenia. *Neuron* 2010; **65**: 585–596.
- 65 Swanson CJ, Kalivas PW. Regulation of locomotor activity by metabotropic glutamate receptors in the nucleus accumbens and ventral tegmental area. *J Pharm Exp Ther* 2000; **292**: 406–414.
- 66 Hodgson RA, Hyde LA, Guthrie DH, Cohen-Williams ME, Leach PT, Kazdoba TM *et al*. Characterization of the selective mGluR1 antagonist, JNJ16259685, in rodent models of movement and coordination. *Pharmacol Biochem Behav* 2011; **98**: 181–187.
- 67 Balu DT, Coyle JT. Neuroplasticity signaling pathways linked to the pathophysiology of schizophrenia. *Neurosci Biobehav Rev* 2011; **35**: 848–870.
- 68 Laruelle M, Kegeles LS, Abi-Dargham A. Glutamate, dopamine, and schizophrenia: from pathophysiology to treatment. *Ann NY Acad Sci* 2003; **1003**: 138–158.
- 69 Perez-Costas E, Melendez-Ferro M, Roberts RC. Basal ganglia pathology in schizophrenia: dopamine connections and anomalies. *J Neurochem* 2010; **113**: 287–302.

- 70 Perez-Costas E, Melendez-Ferro M, Rice MW, Conley RR, Roberts RC. Dopamine pathology in schizophrenia: analysis of total and phosphorylated tyrosine hydroxylase in the substantia nigra. *Front Psychiatry* 2012; **3**: 1–14.
- 71 Yoon JH, Minzenberg MJ, Raouf S, D'Esposito M, Carter CS. Impaired prefrontal-basal ganglia functional connectivity and substantia nigra hyperactivity in schizophrenia. *Biol Psychiatry* 2013; **74**: 122–129.
- 72 Heckers S, Konradi C. Substantia nigra hyperactivity in schizophrenia. *Biol Psychiatry* 2013; **74**: 82–83.
- 73 Reid MA, Kraguljac NV, Avsar KB, White DM, den Hollander JA, Lahti AC. Proton magnetic resonance spectroscopy of the substantia nigra in schizophrenia. *Schizophr Res* 2013; **147**: 348–354.
- 74 Miyake N, Thompson J, Skinbjerg M, Abi-Dargham A. Presynaptic dopamine in schizophrenia. *CNS Neurosci Ther* 2011; **17**: 104–109.
- 75 Lesage A, Steckler T. Metabotropic glutamate mGlu1 receptor stimulation and blockade: therapeutic opportunities in psychiatric illness. *Eur J Pharmacol* 2010; **639**: 2–16.
- 76 Shigemoto R, Nakanishi S, Mizuno N. Distribution of the mRNA for a metabotropic glutamate receptor (mGluR1) in the central nervous system: an in situ hybridization study in adult and developing rat. *J Comp Neurol* 1992; **322**: 121–135.
- 77 Martin LJ, Blackstone CD, Hagan RL, Price DL. Cellular localization of a metabotropic glutamate receptor in rat brain. *Neuron* 1992; **9**: 259–270.
- 78 Lavreysen H, Pereira SN, Leysen JE, Langlois X, Lesage AS. Metabotropic glutamate 1 receptor distribution and occupancy in the rat brain: a quantitative autoradiographic study using [3H]R214127. *Neuropharmacology* 2004; **46**: 609–619.
- 79 Ayoub MA, Angelicheva D, Vile D, Chandler D, Morar B, Cavanaugh JA *et al*. Deleterious GRM1 mutations in schizophrenia. *PLoS One* 2012; **7**: 1–8.
- 80 Gupta DS, McCullumsmith RE, Beneyto M, Haroutunian V, Davis KL, Meador-Woodruff JH. Metabotropic glutamate receptor protein expression in the prefrontal cortex and striatum in schizophrenia. *Synapse* 2005; **57**: 123–131.
- 81 Volk DW, Egan SM, Lewis DA. Alterations in metabotropic glutamate receptor 1 $\alpha$  and regulator of G protein signaling 4 in the prefrontal cortex in schizophrenia. *Am J Psychiatry* 2010; **167**: 1489–1498.
- 82 Brody SA, Conquet F, Geyer MA. Disruption of prepulse inhibition in mice lacking mGluR1. *Eur J Neurosci* 2003; **8**: 2261–3366.
- 83 Selvaraj S, Sun Y, Watt JA, Wang S, Lei S, Birnbaumer L *et al*. Neurotoxin-induced ER stress in mouse dopaminergic neurons involves downregulation of TRPC1 and inhibition of AKT/mTOR signaling. *J Clin Invest* 2012; **122**: 1354–1367.